A refined sine-based finite element with transverse normal deformation for the analysis of laminated beams under thermomechanical loads

P. Vidal, O. Polit

JOURNAL OF MECHANICS OF MATERIALS AND STRUCTURES
Vol. 4, No. 6, 2009

A REFINED SINE-BASED FINITE ELEMENT WITH TRANSVERSE NORMAL DEFORMATION FOR THE ANALYSIS OF LAMINATED BEAMS UNDER THERMOMECHANICAL LOADS

PHILIPPE VIDAL AND OLIVIER POLIT

In the framework of a sine model family, two new three-node beam finite elements including the transverse normal effect are designed for the analysis of laminated beams. They are based on a sine distribution with layer refinement and a second-order expansion for the deflection. The transverse shear strain is obtained using a cosine function, avoiding the use of shear correction factors. This kinematics accounts for the interlaminar continuity conditions on the interfaces between layers, and the boundary conditions on the upper and lower surfaces of the beam. A conforming FE approach is carried out using Lagrange and Hermite interpolations. It is important to notice that the number of unknowns is independent of the number of layers.

Both mechanical and thermomechanical tests for thin and thick beams are presented in order to evaluate the capability of these new finite elements to give accurate results with respect to elasticity or finite element reference solutions. Both convergence velocity and accuracy are discussed and this new finite element yields very satisfactory results at a low computational cost. In particular, the transverse stress computed from the constitutive relation is well estimated with regards to classical equivalent single layer models. This work focuses on the necessity to take into account the transverse normal stress, especially for thick beam and coupled analysis.

1. Introduction

Composite and sandwich structures are widely used in industry due to their excellent mechanical properties, especially their high specific stiffness and strength. In this context, they can be subjected to severe mechanical and thermal conditions (through heating or cooling). For composite design, an accurate knowledge of displacements and stresses is required. Hence it is important to take into account the effects of transverse shear deformation due to a low ratio of transverse shear modulus to axial modulus, or failure due to delamination. In fact, such effects can play an important role in the behavior of structures, and it is desirable to evaluate precisely their influence on local stress fields in each layer, particularly on the interface between layers.

The aim of this paper is to develop two finite elements including the transverse normal deformation, so as to obtain accurate predictions for the behavior of laminated composite beams subjected to mechanical and thermal loading. This analysis is limited to the elasticity area in relation to small displacements. In this context, we put the emphasis on the need to take into account the transverse normal effect, in particular for thermal conditions and for thick structures.

Several theories exist in the mechanics literature for composite or sandwich structures (beams and

Keywords: finite element methods, composites, refined sine-based, layer refinement, transverse normal stress, thermal effects.

plates for the present scope). They have been extended to thermomechanical problems as well. The following classification is associated with the dependence on the number of degrees of freedom (DOFs) with respect to the number of layers:

- The equivalent single layer approach (ESL): the number of unknowns is independent of the number of layers, but continuity of transverse shear and normal stresses is often violated at layer interfaces. The first work for one-layer isotropic plates was proposed in [Basset 1890]. Then, we can distinguish classical laminate theory [Tanigawa et al. 1989] (based on the Euler–Bernoulli hypothesis and leading to inaccurate results for composites and moderately thick beams, because both transverse shear and normal strains are neglected), first-order shear deformation theory [Mindlin 1951] (for composite laminates see [Yang et al. 1966]), and higher-order theories [Librescu 1967; Whitney and Sun 1973; Lo et al. 1977; Reddy 1984].

  In this family, some studies take into account transverse normal deformation. A nonconstant polynomial expression for the out-of-plane displacement is considered in [Kant et al. 1997; Cook and Tessler 1998; Barut et al. 2001; Kant and Swaminathan 2002; Matsunaga 2002; Rao and Desai 2004; Subramanian 2006; Swaminathan and Patil 2007] with a higher-order theory. Specific functions such as the exponential are also used [Soldatos and Watson 1997; Liu and Soldatos 2002]. All these studies are based on a displacement approach, although other approaches are formulated on the basis of mixed formulations [Carrera 2000b; Kim and Cho 2007]. The finite element method is also applied [Kant and Gupta 1988; Vinayak et al. 1996; Subramanian 2001; Zhang and Kim 2005]. In the framework of thermomechanical problems, different approaches have been developed, including mixed formulations [Tessler et al. 2001] and displacement-based ones [Rolfes et al. 1998; Ali et al. 1999; Rohwer et al. 2001; Robaldo 2006].

- The layerwise approach (LW): the number of DOFs depends on the number of layers. This theory aims at overcoming the ESL shortcoming of allowing discontinuity of out-of-plane stresses on the interface layers. It was introduced in [Heller and Swift 1971; Swift and Heller 1974], and also used in [Pagano 1969; Whitney 1969; Srinivas 1973]. For recent contributions, see [Reddy 1989; Shimpi and Ainapure 2001; Kärger et al. 2006]. A mixed formulation also exists [Mau 1973; Murakami 1986].

  Again, some models taking into account the transverse normal effect have been developed: [Icardi 2001; Pai and Palazotto 2001] within a displacement based approach and [Carrera 1999; 2000b; 2004; Rao and Desai 2004] within a mixed formulation. For the thermomechanical analysis, readers can refer to [Robaldo 2006] (displacement) and [Carrera 2000a; Gherlone and di Sciuva 2007] (mixed).

In this framework, refined models have been developed in order to improve the accuracy of ESL models while avoiding the computational burden of the LW approach. Based on physical considerations and after some algebraic transformations, the number of unknowns becomes independent of the number of layers. Whitney [1969] has extended the work of Ambartsumyan [1969] for symmetric laminated composites with arbitrary orientation and a quadratic variation of the transverse stresses in each layer. A family of models, called zig-zag models, was first employed in [di Sciuva 1986], then in [Bhaskar and Varadan 1989; Lee et al. 1992; Cho and Parmerter 1993]. More recently, it was modified and improved in [Gaudenzi et al. 1995; Averill and Yip 1996; Aitharaju and Averill 1999; di Sciuva and Icardi 2001; Kapuria et al. 2003; Gherlone and di Sciuva 2007] with different-order kinematics assumptions, taking into account transverse normal strain.

Another way to improve the accuracy of results consists in the sublaminates strategy, which is proposed in [Flanagan 1994; Averill and Yip 1996]. The number of subdivisions of the laminate thickness determines the accuracy of the approach. It allows localization of the layer refinement without increasing the order of approximation. Nevertheless, the computational cost increases with the number of numerical layers. For recent studies, the reader can also refer to [Icardi 2001; Rao and Desai 2004; Gherlone and di Sciuva 2007].

The literature just cited deals with only some aspects of the broad research activity about models for layered structures and corresponding finite element formulations. An extensive assessment of different approaches has been made in [Noor and Burton 1990; Reddy 1997; Carrera 2002; 2003; Zhang and Yang 2009]. About the particular point of the evaluation of transverse normal stresses, see [Kant and Swaminathan 2000; Mittelstedt and Becker 2007].

In this work, two new finite elements for rectangular laminated beam analysis are built, in order to have a low cost tool that is efficient and simple to use. Our approach is associated with ESL theory. The elements are totally free of shear locking and are based on a refined shear deformation theory [Touratier 1992a] avoiding the use of shear correction factors for laminates. They are based on the sine model of [Ganapathi et al. 1999]. The important new feature is the capability of the model to include the transverse normal effect. So, the transverse displacement is written under a second-order expansion which avoids the Poisson locking mechanism [Carrera and Brischetto 2008]. For the in-plane displacement, the double superposition hypothesis from [Li and Liu 1997] is used: three local functions are added to the sine model. Finally, this process yields to only six or seven independent generalized displacements. All interface and boundary conditions are exactly satisfied for displacements and transverse shear stress. Therefore, this approach takes into account physical meaning.

As far as the interpolation of these finite elements is concerned, our elements are C^0-continuous except for the transverse displacement associated with bending, which is C^1.

We now outline the remainder of this article. First the mechanical formulation for the different models is described. For each of these approaches, the associated finite element is given. They are illustrated by numerical tests performed upon various laminated and sandwich beams. A parametric study is given to show the effects of different parameters such as the length-to-thickness ratio and the number of DOFs. The accuracy of computations is also evaluated by comparison with an exact 3D theory for laminates in bending [Pagano 1969; Ali et al. 1999] and also 2D finite element computations using commercial software. We put the emphasis on the direct calculation of the transverse shear stress from the constitutive relations. The results of our model are then compared with the approach consisting in calculating transverse shear stresses from the equilibrium equations, as in [Chaudhri 1986; Barbero et al. 1990; Vinayak et al. 1996; Liu and Soldatos 2002; Kapuria et al. 2004; Tahani 2007]. In this framework, other approaches are proposed to evaluate transverse shear or normal stresses accurately. Some authors use a hybrid mixed finite element formulation [Han and Hoa 1993] or an iterative predictor-corrector computational procedure [Noor and Malik 1999]. The transverse normal stress is calculated from the integration of the equilibrium equation, avoiding the discontinuity that arises from the use of the constitutive law.

Finally, other numerical examples are presented to demonstrate the effectiveness of the proposed finite elements in coupled analysis. Computations for thick and thin beams of laminated composites are compared to exact 2D elasticity solutions under thermomechanical loading.

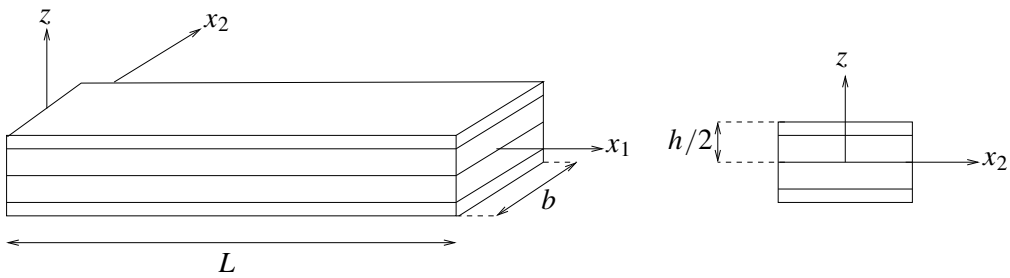

Figure 1. The laminated beam and coordinate system.

2. Resolution of the thermomechanical problem

The governing equations for thermomechanics. Let us consider a beam occupying the domain

$$\mathcal{B} = [0, L] \times \left[-\frac{h}{2} \le z \le \frac{h}{2}\right] \times \left[-\frac{b}{2} \le x_2 \le \frac{b}{2}\right]$$

in a Cartesian coordinate (x_1, x_2, z). The beam has a rectangular uniform cross section of height h and width b and is assumed to be straight. The beam is made of NC layers of different linearly elastic materials. Each layer may be assumed to be orthotropic in the beam axes. The x_1 axis is taken along the central line of the beam whereas x_2 and z are the two axes of symmetry of the cross section intersecting at the centroid, see Figure 1. As shown in this figure, the x_2 axis is along the width of the beam. This work is based upon a displacement approach for geometrically linear elastic beams.

Constitutive relation. Each layer of the laminate is assumed to be orthotropic. Using matrix notation, the thermoelastic stress-strain law of the k-th layer is given by

$$\begin{bmatrix} \sigma_{11}^{(k)} \\ \sigma_{33}^{(k)} \\ \sigma_{13}^{(k)} \end{bmatrix} = \begin{bmatrix} C_{11}^{(k)} & C_{13}^{(k)} & 0 \\ & C_{33}^{(k)} & 0 \\ \text{symmetric} & & C_{55}^{(k)} \end{bmatrix} \begin{bmatrix} \varepsilon_{11}^{(k)} - \alpha_{11}^{(k)} \Delta T \\ \varepsilon_{33}^{(k)} - \alpha_{33}^{(k)} \Delta T \\ \varepsilon_{13}^{(k)} \end{bmatrix}, \quad \text{that is, } [\sigma^{(k)}] = [C^{(k)}][\varepsilon^{(k)}], \tag{1}$$

where ΔT is the temperature rise, $[\sigma]$ is the stress tensor, $[\varepsilon]$ is the strain tensor, the C_{ij} are the 3D stiffness coefficients, and α_{ij} are the thermal expansion coefficients obtained after a transformation from the material axes to the Cartesian coordinate system.

The weak form of the boundary value problem. Using the above matrix notation and for admissible virtual displacement $\vec{u}^* \in U^*$, the variational principle is this:

Find $\vec{u}$ in the space U of admissible displacements such that

$$-\int_{\mathcal{B}} [\varepsilon(\vec{u}^*)]^T [\sigma(\vec{u})] d\mathcal{B} + \int_{\mathcal{B}} [u^*]^T [f] d\mathcal{B} + \int_{\partial\mathcal{B}_F} [u^*]^T [F] d\partial\mathcal{B} = \int_{\mathcal{B}} \rho [u^*]^T [\ddot{u}] d\mathcal{B}, \quad \forall \vec{u}^* \in U^*, \tag{2}$$

where $[f]$ and $[F]$ are the prescribed body and surface forces applied on $\partial\mathcal{B}_F$, $\varepsilon(\vec{u}^*)$ is the virtual strain, and ρ is the mass density.

Equation (2) is a classical starting point for finite element approximations.

The displacement field for laminated beams. Based on the sine function [Touratier 1991; Dau et al. 2006], we now present two models that take into account transverse normal deformation:

- SinRef-6p, a refined sine model with second-order expansion for the transverse displacement and the refinement added in each layer; and
- SinRef-7p, a refined sine model with one more unknown than SinRef-6p for in-plane displacement.

These models are based on

- works on beams, plates and shells such as [Ganapathi et al. 1999; Touratier 1991; 1992a; 1992b; Polit and Touratier 2002; Vidal and Polit 2006; 2009], covering the refined theory, and
- the so-called 1,2-3 double-superposition theory of [Li and Liu 1997].

It also follows the local-global approach studied in [Sze et al. 1998; Wu et al. 2005; Zhen and Wanji 2007].

These refined models (see [Vidal and Polit 2008]) take into account the continuity conditions between layers of the laminate for both displacements and transverse shear stress, and the free conditions on the upper and lower surfaces owing to the Heaviside function.

The kinematics of the two models is assumed to be of the following particular form, where the prime stands for differentiation with respect to x_1 and H is the Heaviside step function ($H(z) = 1$ if $z \geq 0$ and $H(z) = 0$ otherwise):

1. The 6-parameter SinRef-6p model:

$$\begin{cases} u_1(x_1, x_2, z) = u(x_1) - z w_0(x_1)' + f(z)(\omega_3(x_1) + w_0(x_1)') \\ \qquad\qquad + \displaystyle\sum_{k=1}^{NC} \big(\bar{u}_{\text{loc}}^{(k)}(x_1, z) + \hat{u}_{\text{loc}}^{(k)}(x_1, z)\big)(H(z - z_k) - H(z - z_{k+1})), \\ u_3(x_1, x_2, z) = w_0(x_1) + z w_1(x_1) + z^2 w_2(x_1). \end{cases} \tag{3}$$

2. The 7-parameter SinRef-7p model:

$$\begin{cases} u_1(x_1, x_2, z) = u(x_1) + z v(x_1) + f(z)(\omega_3(x_1) + w_0(x_1)') \\ \qquad\qquad + \displaystyle\sum_{k=1}^{NC} \big(\bar{u}_{\text{loc}}^{(k)}(x_1, z) + \hat{u}_{\text{loc}}^{(k)}(x_1, z)\big)(H(z - z_k) - H(z - z_{k+1})), \\ u_3(x_1, x_2, z) = w_0(x_1) + z w_1(x_1) + z^2 w_2(x_1). \end{cases} \tag{4}$$

In the classic approach, w_0 is the bending deflection following the z direction, while u is associated with the uniform extension of the cross section of the beam along the central line, and ω_3 is the shear bending rotation around the z axis.

Note that the kinematic constraint concerning the relation with the derivative of the deflection ($v(x_1) = -w_0(x_1)_{,1}$) is relaxed in the SinRef-7p model.

The local functions $\bar{u}_{\text{loc}}^{(k)}$ and $\hat{u}_{\text{loc}}^{(k)}$ are based on the first few Legendre polynomials, which are $A_1(\zeta) = \zeta$, $A_2(\zeta) = -\frac{1}{2} + \frac{3}{2}\zeta^2$, and $A_3(\zeta) = -\frac{3}{2}\zeta + \frac{5}{2}\zeta^3$. They can be written as

$$\bar{u}_{\text{loc}}^{(k)}(x_1, z) = A_1(\zeta_k) u_{31}^k(x_1) + A_2(\zeta_k) u_{32}^k(x_1), \qquad \hat{u}_{\text{loc}}^{(k)}(x_1, z) = A_3(\zeta_k^3) u_{33}^k(x_1), \tag{5}$$

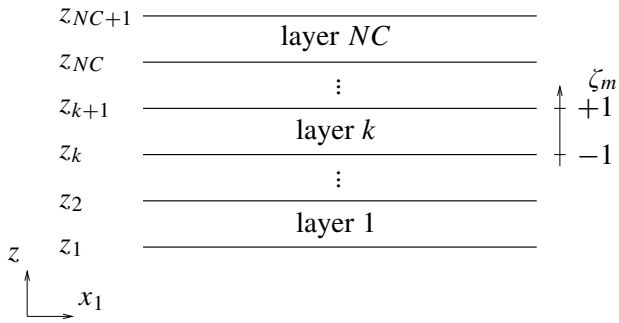

Figure 2. Transverse coordinate of the laminated beam.

where we have introduced the nondimensional coordinate

$$\zeta_k = a_k z - b_k, \qquad \text{with} \quad a_k = \frac{2}{z_{k+1} - z_k} \quad \text{and} \quad b_k = \frac{z_{k+1} + z_k}{z_{k+1} - z_k} \tag{6}$$

(see Figure 2). Legendre polynomials are orthogonal over the interval $[-1, 1]$ to constants and to each other — that is, $\int_{-1}^{1} A_i(\zeta_k)\, d\zeta_k = 0$ for $i = 1, 2, 3$ and $\int_{-1}^{1} A_i(\zeta_k) A_j(\zeta_k) d\zeta_k = 0$ for $i \neq j$.

From (3), classical beam models can be deduced without the local functions and the two higher-order terms of the transverse displacement:

- Euler–Bernoulli: $f(z) = 0$,
- Timoshenko: $f(z) = z$,
- sine model: $f(z) = \dfrac{h}{\pi} \sin \dfrac{\pi z}{h}$.

The derivative of this last function will represent the transverse shear strain distribution due to bending. Note that it is not necessary to introduce transverse shear correction factors because the two models in this work predict the shear energy sufficiently accurately, thanks to the higher-order kinematic assumptions.

At this stage, $3 \times NC + 5$ generalized displacements are included in the SinRef-6p model and $3 \times NC + 6$ in the SinRef-7p model; see (3)+(5) and (4)+(5), respectively.

We next turn to the task of deriving relations between the kinematic unknowns from

- lateral boundary conditions, and
- interlaminar continuity conditions (displacement, transverse shear stress).

In the following, we only focus on the SinRef-7p model. The same procedure can be carried out for the SinRef-6p model by setting $v(x_1) = -w_0(x_1)_{,1}$.

Continuity conditions and free conditions. From the displacement field (4), continuity conditions on displacements and the interlaminar stress must be imposed. For an interface layer $k \in \{2, \ldots, NC\}$, we have:

- Displacement continuity conditions as in [Sze et al. 1998]:

$$\begin{aligned} \bar{u}^{(k)}_{\text{loc}}(x_1, z_k) &= \bar{u}^{(k-1)}_{\text{loc}}(x_1, z_k), \qquad k = 2, \ldots, NC, \\ \hat{u}^{(k)}_{\text{loc}}(x_1, z_k) &= \hat{u}^{(k-1)}_{\text{loc}}(x_1, z_k), \qquad k = 2, \ldots, NC. \end{aligned} \tag{7}$$

- Transverse shear stress continuity between two adjacent layers:

$$\sigma_{13}^{(k)}(x_1, z_k^+) = \sigma_{13}^{(k-1)}(x_1, z_k^-), \qquad k = 2, \ldots, NC. \tag{8}$$

So, $3 \times (NC - 1)$ conditions are imposed, which allows us to reduce the number of unknowns to 9 generalized displacements.

Free conditions of the transverse shear stress on the upper and lower surfaces must also be verified. So, we have

$$\sigma_{13}^{(1)}\left(x_1, z = -\frac{h}{2}\right) = 0, \qquad \sigma_{13}^{(NC)}\left(x_1, z = \frac{h}{2}\right) = 0. \tag{9}$$

Finally, the number of generalized displacements is reduced to 7, which is independent from the number of layers.

Relation between the generalized displacements. Using the notations introduced in (5), the conditions (7)–(9) can be written in the following form:

$$[A]\{v\} = \{b\}u_{31}^1(x_1) + \{c\}(\omega_3(x_1) + w_0(x_1)') + \{d\}(v(x_1) + w_0(x_1)') + \{e\}w_1(x_1)' + \{f\}w_2(x_1)', \tag{10}$$

where $[A]$ is a $(3\,NC - 1) \times (3\,NC - 1)$ matrix, and $\{b\}$, $\{c\}$, $\{d\}$, $\{e\}$, $\{f\}$, and

$$\{v\}^T = \left\{u_{32}^1 \;\; u_{33}^1 \;\; \vdots \;\; u_{31}^j \;\; u_{32}^j \;\; u_{33}^j \;\; \vdots \;\; u_{31}^{NC} \;\; u_{32}^{NC} \;\; u_{33}^{NC}\right\}^T$$

are vectors with $3\,NC - 1$ components.

From the resolution of this linear system, relations between u_{31}^j ($j \neq 1$), u_{32}^j, u_{33}^j, $j = 1, \ldots, NC$, and u_{31}^1 can be deduced. This relation can be written in the following form:

$$\begin{aligned} u_{3i}^j(x_1) = {} & \beta_i^j\left(\omega_3(x_1) + w_0(x_1)'\right) + \eta_i^j\left(v(x_1) + w_0(x_1)'\right) \\ & + \delta_i^j u_{31}^1(x_1) + \lambda_i^j w_1(x_1)' + \mu_i^j w_2(x_1)', \quad j = 1, \ldots, NC, \quad i = 1, 2, 3, \end{aligned} \tag{11}$$

with $\delta_1^1 = 1$ and $\beta_1^1 = \eta_1^1 = \lambda_1^1 = \mu_1^1 = 0$, and where β_i^j, δ_i^j, λ_i^j, μ_i^j, and η_i^j ($i = 1, 2, 3$) are the coefficients deduced from (10).

Finally, the 7 unknowns become u, w_0, ω_3, v, w_1, w_2, and u_{31}^1. It is noted that the SinRef-6p model involves 6 unknowns (u, w_0, ω_3, w_1, w_2, and u_{31}^1).

Expression of strains. Matrix notation can be easily defined using a generalized displacement vector as

$$[u]^T = [F_u(z)][\mathscr{E}_u], \quad [\mathscr{E}_u]^T = \left[u \;\cdots\; w_0 \; w_{0,1} \;\cdots\; \omega_3 \;\cdots\; u_{31}^1 \;\cdots\; v \;\cdots\; w_1 \; w_{1,1} \;\cdots\; w_2 \; w_{2,1}\right], \tag{12}$$

and $[F_u(z)]$ depends on the normal coordinate z according to

$$[F_u(z)] = \begin{bmatrix} 1 & 0 & F_{u13}(z) & F_{u14}(z) & F_{u15}(z) & F_{u16}(z) & 0 & F_{u18}(z) & 0 & F_{u110}(z) \\ 0 & 1 & 0 & 0 & 0 & 0 & z & 0 & z^2 & 0 \end{bmatrix}, \tag{13}$$

where

$$\begin{aligned} F_{u13}(z) &= f(z) + S_\beta(z) + S_\eta(z), & F_{u15}(z) &= S_\delta(z), & F_{u18}(z) &= S_\lambda(z), \\ F_{u14}(z) &= f(z) + S_\beta(z), & F_{u16}(z) &= z + S_\eta(z), & F_{u110}(z) &= S_\mu(z), \end{aligned}$$

and

$$S_\beta(z)=\sum_{k=1}^{NC}\left(\zeta_k\beta_1^k+\left(-\tfrac{1}{2}+\tfrac{3}{2}\zeta_k^2\right)\beta_2^k+\left(-\tfrac{3}{2}\zeta_k+\tfrac{5}{2}\zeta_k^3\right)\beta_3^k\right)\Delta H(k,k+1),$$

$$S_\delta(z)=\sum_{k=1}^{NC}\left(\zeta_k\delta_1^k+\left(-\tfrac{1}{2}+\tfrac{3}{2}\zeta_k^2\right)\delta_2^k+\left(-\tfrac{3}{2}\zeta_k+\tfrac{5}{2}\zeta_k^3\right)\delta_3^k\right)\Delta H(k,k+1),$$

$$S_\eta(z)=\sum_{k=1}^{NC}\left(\zeta_k\eta_1^k+\left(-\tfrac{1}{2}+\tfrac{3}{2}\zeta_k^2\right)\eta_2^k+\left(-\tfrac{3}{2}\zeta_k+\tfrac{5}{2}\zeta_k^3\right)\eta_3^k\right)\Delta H(k,k+1),$$

$$S_\lambda(z)=\sum_{k=1}^{NC}\left(\zeta_k\lambda_1^k+\left(-\tfrac{1}{2}+\tfrac{3}{2}\zeta_k^2\right)\lambda_2^k+\left(-\tfrac{3}{2}\zeta_k+\tfrac{5}{2}\zeta_k^3\right)\lambda_3^k\right)\Delta H(k,k+1),$$

$$S_\mu(z)=\sum_{k=1}^{NC}\left(\zeta_k\mu_1^k+\left(-\tfrac{1}{2}+\tfrac{3}{2}\zeta_k^2\right)\mu_2^k+\left(-\tfrac{3}{2}\zeta_k+\tfrac{5}{2}\zeta_k^3\right)\mu_3^k\right)\Delta H(k,k+1),$$

with $\Delta H(k,k+1)=H(z-z_k)-H(z-z_{k+1})$.

The strains for the laminated beam are

$$\begin{aligned}
\varepsilon_{11}&=u_{,1}+zv_{,1}+(f(z)+S_\beta(z))(w_{0,11}+\omega_{3,1})+S_\delta(z)u^1_{31,1}\\
&\qquad+S_\lambda(z)w_{1,11}+S_\mu(z)w_{2,11}+S_\eta(z)(w_{0,11}+v_{,1}),\\
\varepsilon_{33}&=w_1+2zw_2,\\
\gamma_{13}&=(f(z)_{,3}+S_\beta(z)_{,3})(w_{0,1}+\omega_3)+S_\delta(z)_{,3}u^1_{31}\\
&\qquad+(0+S_\eta(z)_{,3})(w_{0,1}+v)+(z+S_\lambda(z)_{,3})w_{1,1}+(z^2+S_\mu(z)_{,3})w_{2,1}.
\end{aligned}\tag{14}$$

These expressions can be described in matrix notation by

$$[\varepsilon]=[F_s(z)][\mathscr{C}_s],$$

$$[\mathscr{C}_s]^T=\left[u_{,1}\ \vdots\ w_{0,1}\ w_{0,11}\ \vdots\ \omega_3\ \omega_{3,1}\ \vdots\ u^1_{31}\ u^1_{31,1}\ \vdots\ v\ v_{,1}\ \vdots\ w_1\ w_{1,1}\ w_{1,11}\ \vdots\ w_2\ w_{2,1}\ w_{2,11}\right],\tag{15}$$

and $[F_s(z)]$ depends on the normal coordinate z as

$$[F_s(z)]=\begin{bmatrix}
1 & 0 & f(z)+S_\beta(z)+S_\eta(z) & 0 & \dots\\
0 & 0 & 0 & 0 & \dots\\
0 & 1+\left(f(z)_{,3}+S_\beta(z)_{,3}+S_\eta(z)_{,3}\right) & 0 & \left(f(z)_{,3}+S_\beta(z)_{,3}\right) & \dots
\end{bmatrix}$$

$$\begin{bmatrix}
\left(f(z)+S_\beta(z)\right) & 0 & S_\delta(z) & 0 & z+S_\eta(z) & 0 & 0 & S_\lambda(z) & 0 & 0 & S_\mu(z)\\
0 & 0 & 0 & 0 & 0 & 1 & 0 & 0 & 2z & 0 & 0\\
0 & S_\delta(z)_{,3} & 0 & 1+S_\eta(z)_{,3} & 0 & 0 & z+S_\lambda(z)_{,3} & 0 & 0 & z^2+S_\mu(z)_{,3} & 0
\end{bmatrix}.\tag{16}$$

Matrix expression for the weak form. From the weak form of the boundary value problem (2), and using (15) and (16), an integration throughout the cross-section is performed analytically in order to obtain an unidimensional formulation. Therefore, the first left term of (2) can be written in the following form:

$$\int_{\mathscr{B}}[\varepsilon(\vec{u}^*)]^T[\sigma(\vec{u})]d\mathscr{B}=\int_0^L[\mathscr{C}_s^*]^T[k][\mathscr{C}_s]dx_1,\qquad[k]=\int_\Omega[F_s(z)]^T[C][F_s(z)]d\Omega,\tag{17}$$

where $[C]$ is the constitutive law given on page 1130 and Ω represents the cross-section

$$\left[-\frac{h}{2}\le z\le\frac{h}{2}\right]\times\left[-\frac{b}{2}\le x_2\le\frac{b}{2}\right].$$

Figure 3. Description of the laminated beam finite element DOF. SinRef-6p (left) and SinRef-7p (right).

In (17), the matrix $[k]$ is the integral of the beam's material characteristics throughout the cross-section. An advantage of the Legendre polynomials is the easy calculation of the matrices $[k]$, arising from orthogonality (page 1132).

The finite element approximation. This section is devoted to the finite element approximation of the generalized displacement, see the matrices $[\mathscr{E}_s]$, $[\mathscr{E}_s^*]$, $[\mathscr{E}_u]$, and $[\mathscr{E}_u^*]$ from (15) and (12). We describe it briefly; for details see [Ganapathi et al. 1999; Vidal and Polit 2008].

The geometric approximation. Given the displacement field constructed above for sandwich and laminated beams, a corresponding finite element is developed in order to analyze the behavior of laminated beam structures under combined loads. Let us consider the e-th element ${L_e}^h$ of the mesh $\bigcup {L_e}^h$. This element has three nodes, denoted by $(g_j)_{j=1,2,3}$, see Figure 3. The coordinate x_1 of a point on the central line of the beam is approximated by

$$x_1(\xi) = \sum_{j=1}^{2} Nl_j(\xi) {x_1}^e(g_j), \tag{18}$$

where the $Nl_j(\xi)$ are Lagrange linear interpolation functions and the ${x_1}^e(g_j)$ are Cartesian coordinates (measured along the x_1 axis) of node g_j of element ${L_e}^h$. The isoparametric or reduced coordinate ξ ranges in the interval $[-1, 1]$.

Interpolation for the bending-traction beam element. The finite element approximations of the assumed displacement field components are hereafter symbolically written as ${u_i}^h(x_1, x_2, z)$ where the superscript h refers to the mesh $\bigcup {L_e}^h$.

The kinematic equation (4) states that the transverse displacement w_0^h must be C^1-continuous; the rotation angle ${\omega_3}^h$, the extension displacement u^h, and the variables v^h and u_{31}^1 might be only C^0-continuous. Therefore, the generalized displacements w_0^h, w_1^h, and w_2^h are interpolated by the Hermite cubic functions $Nh_j(\xi)$.

According to the transverse shear locking condition, the other shear bending generalized displacements and the rotation angle ${\omega_3}^h$ are interpolated by Lagrange quadratic functions, denoted by $Nq_j(\xi)$. This choice allows the same order of interpolation for both $w_{0,1}^h$ and ${\omega_3}^h$ in the corresponding transverse shear strain components due to bending, thus avoiding transverse shear locking according to the field compatibility approach [Polit et al. 1994].

Finally, the generalized displacements u^h, v^h, u_{31}^1 are interpolated by Lagrange quadratic functions.

Elementary matrices. Having defined all the finite element mechanical approximations, we can now deduce the elementary stiffness matrix $[K^e_{uu}]$ from (17). It has the expression

$$[K^e_{uu}] = \int_{L_e} [B]^T [k][B] dL_e, \tag{19}$$

where $[B]$ is deduced from the relation between the generalized displacement vectors (15) and the elementary vector of DOFs, denoted by $[q_e]$:

$$[\mathscr{E}_s] = [B][q_e]. \tag{20}$$

The matrix $[B]$ contains only the derivatives of the interpolation functions and the Jacobian components. The same technique can be used to define the elementary mechanical load vector, denoted $[B^e_u]$, but it is not detailed here.

3. Results and discussion

In this section, several static tests are presented validating our finite element and evaluating its efficiency. The influence of transverse normal stress is also discussed and evaluated through the integration of the equilibrium equation. Then, a thermomechanical problem is carried out.

Mechanical analysis. The aim of our investigation is to study the efficiency of these new elements to analyze the flexural behavior of highly inhomogeneous laminated beams for static mechanical problems under global and localized pressure. The results are compared with those obtained with SinRef-c, the sine model with Heaviside function [Vidal and Polit 2008], which does not take into account the transverse normal effect; and also with reference solutions (the exact solution [Pagano 1969] or a 2D solution calculated with ANSYS). To evaluate the performance of the element in bending, we considered various cases in the next three sections.

Properties of the finite element. Before proceeding to the detailed analysis, numerical computations are carried out for the rank of the element (spurious mode), convergence properties and the effect of aspect ratio (shear locking).

The test concerns simply supported thick symmetric composite beams and is taken from [Pagano 1969]. It is detailed below.

Geometry: Composite cross-ply beam $(0°/90°/0°)$ and length to thickness ratio $S = 4$ $(S = \frac{L}{h})$; half of the beam is meshed. All layers have the same thickness.

Boundary conditions: Simply supported beam subjected to a sinusoidal load $q(x_1) = q_0 \sin \dfrac{\pi x_1}{L}$.

Material properties:

$$E_L = 172.4\,\text{GPa}, \quad E_T = 6.895\,\text{GPa}, \quad G_{LT} = 3.448\,\text{GPa}, \quad G_{TT} = 1.379\,\text{GPa}, \quad \nu_{LT} = \nu_{TT} = 0.25,$$

where L refers to the fiber direction, and T refers to the transverse direction.

This element has a proper rank without any spurious energy modes when exact integration is applied to obtain the stiffness matrix [Ganapathi et al. 1999]. For this purpose, a scheme with three integration points is used. There is also no need to use shear correction factors here, as the transverse strain is represented by a cosine function.

N	number of DOFs	$\bar{w}(L/2,0)$	error	$\bar{\sigma}_{13}(0,0)$ direct	error	equil. eq.	error
1	12	2.8984	0.4%	1.4395	0.6%	0.9404	34%
2	24	2.8897	0.1%	1.4184	0.9%	1.2974	9%
4	48	2.8887	0.1%	1.4168	1%	1.3960	2%
8	96	2.8886	0.0%	1.4167	1%	1.4212	0.7%
16	192	2.8886	0.0%	1.4328	0.1%	1.4421	0.7%

Table 1. $\bar{\sigma}_{13}(0,0)$ and $\bar{w}(L/2,0)$ for different number of DOFs: mesh convergence study, with three layers $(0°/90°/0°)$, $S=4$, SinRef-6p. The word "direct" labels results derived from the constitutive equation, rather than the equilibrium equation.

Table 1 gives the convergence of the SinRef-6p model for the transverse displacement and the transverse shear stress for $S=4$. For this last component, results can be obtained using the constitutive relation (column labeled "direct" with its corresponding percent error), or alternatively using the equilibrium equation at the postprocessing level, that is

$$\sigma_{13}(z) = -\int_{-h/2}^{z} \sigma_{11,1}\, dx_3,$$

(column labeled "equil. eq" and its error). It must be noticed that the deflection is less sensitive to the mesh than the shear stress. The convergence velocity is very high. Based on progressive mesh refinement, a $N=8$ mesh is adequate to model the thick laminated beam for a bending analysis. Moreover, the results obtained with coarse meshes are in good agreement with the reference values. Note that this model gives very good results for the transverse shear stress calculated with the constitutive relation.

Considering various values for the aspect ratio, the normalized displacement obtained at the middle of the simply supported composite beam is shown in Figure 4 along with the exact solution [Pagano 1970], and they are found to be in excellent agreement. It is also inferred from Figure 4 that the present

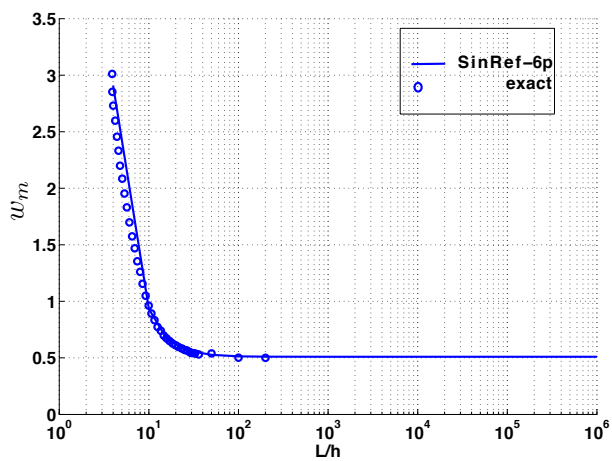

Figure 4. Nondimensional maximum displacement $w_m = 100u_3(L/2,0)E_T h^3/(q_0 L^4)$ versus aspect ratio S, with three layers $(0°/90°/0°)$, mesh $N=8$, SinRef-6p model.

element is free from the shear locking phenomenon as the element is developed using a field compatibility approach.

Bending analysis of laminated composite beam. This test is about simply supported symmetric and antisymmetric composite beams from Reference [Pagano 1970]. It is detailed below.

Geometry: Composite cross-ply beam (0°/90°/0°) and (0°/90°) and length to thickness ratio from $S = 2$ to $S = 40$; half of the beam is meshed. All layers have the same thickness.

Boundary conditions: Simply supported beam subjected to a sinusoidal load $q(x_1) = q_0 \sin \dfrac{\pi x_1}{L}$.

Material properties: Same properties as on page 1136.

Mesh: $N = 8$.

Results: The results ($\bar{u}$, $\bar{w}$, $\bar{\sigma}_{11}$, $\bar{\sigma}_{13}$) are made nondimensional using

$$\bar{u} = \frac{E_T u_1(0, h/2)}{h q_0}, \quad \bar{w} = \frac{100 E_T u_3(L/2, 0)}{S^4 h q_0}, \quad \bar{\sigma}_{11} = \frac{\sigma_{11}(L/2, \pm h/2)}{q_0}, \quad \bar{\sigma}_{13} = \frac{\sigma_{13}(0, 0 \text{ or } -h/4)}{q_0}. \tag{21}$$

The two layer case (0°/90°) is presented first. The numerical results for deflection, in-plane displacement, shear stress, and in-plane stress are given in Tables 2–4 with respect to the span-to-thickness ratio:

			$\bar{u}(0, h/2)$				
S	SinRef-7p	error	SinRef-6p	error	SinRef-c	error	exact
2	0.760	0.3%	0.801	5%	0.848	11%	0.762
4	4.55	0.1%	4.60	1%	4.78	5%	4.55
20	485.22	< 0.1%	485.32	< 0.1%	486.20	0.2%	485.15
40	3856.1	< 0.01%	3856.3	< 0.01%	3858.7	< 0.1%	3856.3
			$\bar{w}(L/2, 0)$				
S	SinRef-7p	error	SinRef-6p	error	SinRef-c	error	exact
2	10.691	1%	10.438	3%	10.5608	2%	10.849
4	4.682	0.2%	4.614	1%	4.696	< 0.1%	4.695
20	2.702	< 0.1%	2.699	0.1%	2.703	< 0.1%	2.703
40	2.639	0.01%	2.638	< 0.1%	2.640	< 0.1%	2.639

Table 2. $\bar{u}(0, h/2)$ and $\bar{w}(L/2, 0)$ for different values of S, with two layers (0°/90°).

	maximum of $\bar{\sigma}_{13}$												
	SinRef-7p				SinRef-6p				SinRef-c				
S	direct	error	equil.eq	error	direct	error	equil.eq	error	direct	error	equil.eq	error	exact
2	1.213	5%	1.112	3%	1.121	3%	1.163	0.6%	1.202	4%	1.248	8%	1.155
4	2.761	2%	2.679	1%	2.546	5%	2.717	0.4%	2.588	4%	2.768	2%	2.706
20	14.709	0.6%	14.540	0.5%	13.463	7%	14.549	0.5%	13.450	8%	14.555	0.5%	14.620
40	29.488	0.5%	29.167	0.5%	26.981	7%	29.172	0.5%	26.940	8%	29.165	0.5%	29.324

Table 3. Maximum value of $\bar{\sigma}_{13}$ for different values of S, with two layers (0°/90°). The maximum occurs at $(0, -h/4)$ for $S = 4, 20, 40$.

	$\bar{\sigma}_{11}(L/2, -h/2)$						
S	SinRef-7p	error	SinRef-6p	error	SinRef-c	error	exact
2	9.9	12%	10.0	13%	11.1	26%	8.8
4	30.8	2%	31.0	3%	31.9	6%	30.0
20	702.7	0.4%	703.1	0.5%	703.5	0.5%	699.7
40	2803.3	0.3%	2803.7	0.4%	2803.1	0.3%	2792.6

Table 4. $\bar{\sigma}_{11}(L/2, -h/2)$ for different values of S, with two layers (0°/90°).

$S = 2$ (very thick), $S = 4$ (thick), $S = 20$ (moderately thick), or $S = 40$ (thin). The percent error with respect to S are also compared in these tables. The variation of the normalized in-plane, transverse shear, and normal stresses, and the transverse displacement through the thickness ($S = 2$, $S = 4$) are presented in Figures 5–7 for further comparison (only the most critical tests).

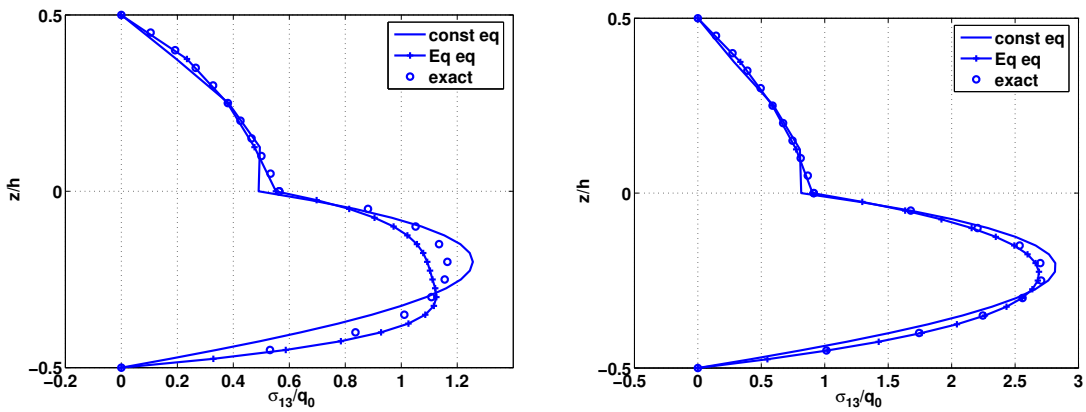

Figure 5. Distribution of $\bar{\sigma}_{13}$ along the thickness, $S = 2$ (left) and $S = 4$ (right), with two layers (0°/90°), SinRef-7p.

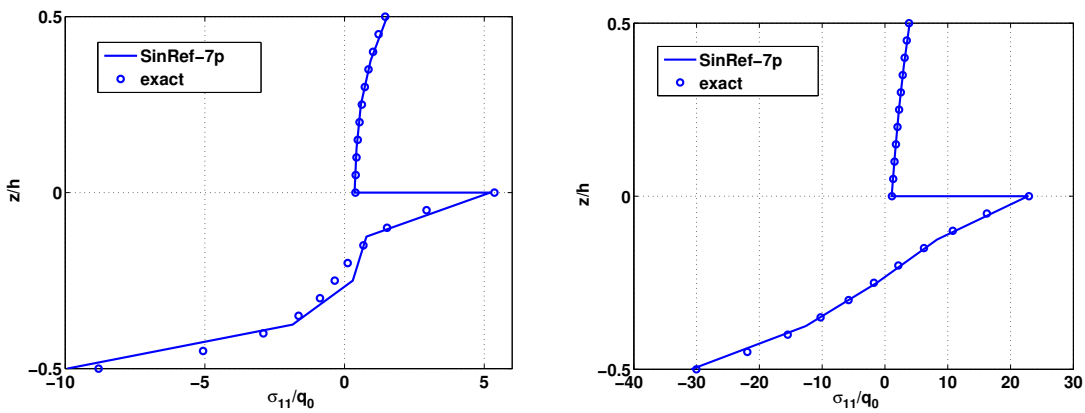

Figure 6. Distribution of $\bar{\sigma}_{11}$ $S = 2$ (left) and $\bar{\sigma}_{11}$ $S = 4$ (right) along the thickness, with two layers (0°/90°), SinRef-7p.

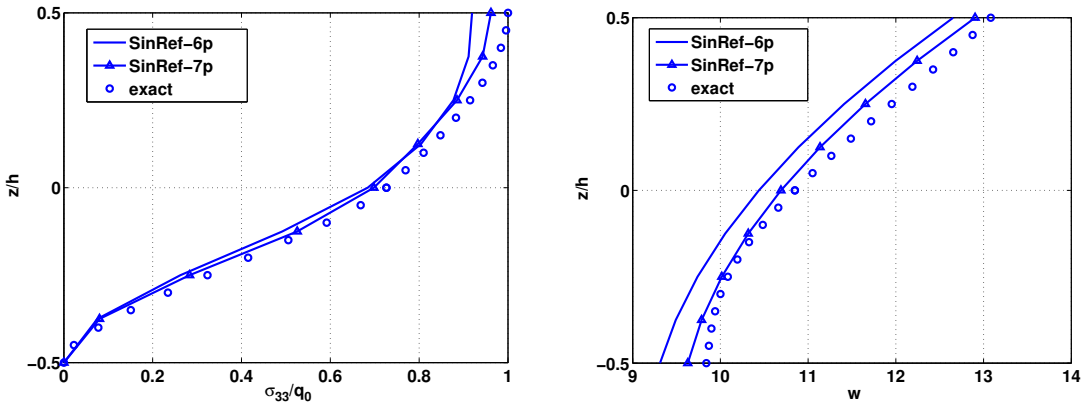

Figure 7. Distribution of $\bar{\sigma}_{33}$ (left) and $\bar{w}$ (right) along the thickness, $S = 2$, with two layers (0°/90°).

For the displacements, the SinRef-7p model gives more precise results than the two other models, especially for the very thick case. For $S \geq 4$, the error is less than 1% for the deflection, and less than 5% for the in-plane displacement regardless of the model. For $S = 2$, the two present models take into account the nonconstant variation through the thickness (see Figure 7, right).

Concerning the stresses, the evolution of the transverse shear stress is improved using one more unknown in the model (see Table 3) but no influence is denoted for the in-plane stress (see Table 4). The effect of the transverse normal stress in the model allows us to improve the accuracy of $\bar{\sigma}_{13}$ and $\bar{\sigma}_{11}$, especially for the very thick beam. For the SinRef-7p model, errors on $\bar{\sigma}_{13}$ calculated from the constitutive law are less than 5%. For the in-plane stress, all the errors are less than 6% for $S \geq 4$.

It is seen from Figures 5–7 that the SinRef-7p element performs very well for thick as well as thin beams (all results are not presented here for brevity). The distribution of the in-plane displacement (not presented here) and stress is similar to the exact Pagano solution regardless of the length-to-thickness ratio. The transverse shear stress obtained using the equilibrium equation gives excellent results, especially for

			$\bar{u}(0, h/2)$				
S	SinRef-7p	error	SinRef-6p	error	SinRef-c	error	exact
2	0.237	8%	0.238	9%	0.204	6%	0.218
4	0.944	0.5%	0.945	0.6%	0.942	0.3%	0.939
20	66.776	0.1%	66.758	0.1%	66.864	< 0.01%	66.869
40	517.88	< 0.1%	517.84	0.04%	518.08	< 0.01%	518.08
			$\bar{w}(L/2, 0)$				
S	SinRef-7p	error	SinRef-6p	error	SinRef-c	error	exact
2	8.505	0.2%	8.488	0.4%	8.746	2%	8.524
4	2.888	< 0.1%	2.888	0.04%	2.908	< 1%	2.887
20	0.617	< 0.01%	0.617	0.01%	0.617	< 0.1%	0.617
40	0.537	< 0.01%	0.537	< 0.01%	0.537	< 0.01%	0.537

Table 5. $\bar{w}(L/2, 0)$ and $\bar{u}(0, h/2)$ for different values of S, with three layers (0°/90°/0°).

$\bar{\sigma}_{13}(0,0)$													
	SinRef-7p				SinRef-6p				SinRef-c				
S	direct	error	equil.eq	error	direct	error	equil.eq	error	direct	error	equil.eq	error	exact
2	0.5328	0.2%	0.5312	0.5%	0.4841	9%	0.5300	0.8%	0.4989	6%	0.5379	0.6%	0.5343
4	1.4303	<0.1%	1.4216	0.7%	1.4167	1%	1.4212	0.7%	1.4213	<1%	1.4236	<1%	1.4318
20	8.7480	<0.01%	8.6965	0.5%	9.006	2.9%	8.697	0.5%	9.0052	2.9%	8.6973	<1%	8.7490
40	17.642	<0.01%	17.539	0.5%	18.186	3%	17.539	0.5%	18.184	3%	17.539	<1%	17.634

Table 6. $\bar{\sigma}_{13}(0,0)$ for different values of S, with three layers $(0°/90°/0°)$.

$\bar{\sigma}_{11}(L/2,h/2)$							
S	SinRef-7p	error	SinRef-6p	error	SinRef-c	error	exact
2	9.70	9%	9.74	9%	8.07	9%	8.90
2 $(-h/2)$	6.96	1.2%	7.01	1.9%	8.07	17%	6.87
4	18.4	2%	19.0	1%	18.6	1%	18.8
20	264.2	0.3%	264.0	$< 0.5\%$	264.0	$< 0.5\%$	263.2
40	1023.2	0.3%	1023.0	$< 0.5\%$	1023.0	$< 0.5\%$	1019.8

Table 7. $\bar{\sigma}_{11}(L/2,h/2)$ for different values of S, with three layers $(0°/90°/0°)$.

the very thick beam with $S = 2$ (see Figure 5). For design applications, the variation of the transverse shear stress deduced from the constitutive relation yields satisfactory distributions even for the very thick beam, without computational cost at the postprocessing level. The accuracy of the transverse normal stress is also very good (see Figure 7, left).

Next we consider the three-layer case $(0°/90°/0°)$. The results are summarized in Tables 5–7. Figures 8–11 (SinRef-7p model) show the transverse normal and shear stresses and out-of-plane displacement. All models give excellent results for $S = 4, 20, 40$. Again, note that the SinRef-7p model improves the accuracy of the results for both displacements and transverse shear stresses especially for thick laminates.

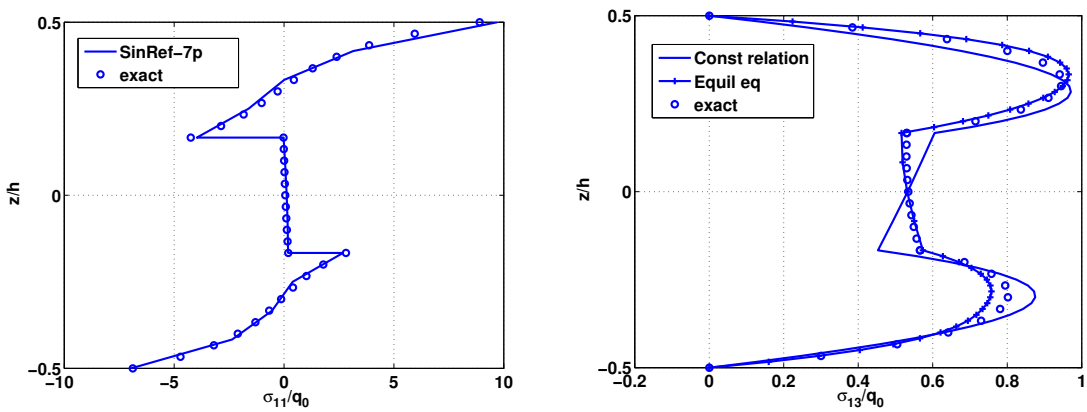

Figure 8. Distribution of $\bar{\sigma}_{13}$ along the thickness, $S = 2$, with three layers $(0°/90°/0°)$, SinRef-7p.

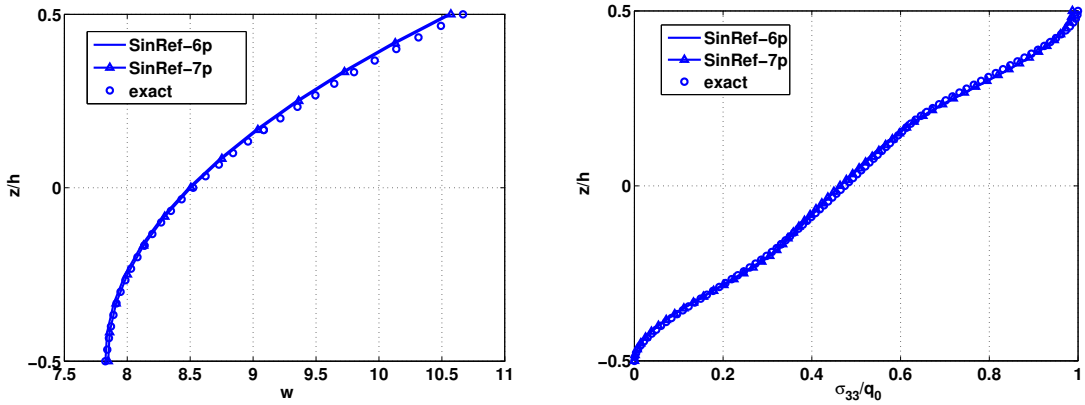

Figure 9. Distribution of $\bar{w}$ and $\bar{\sigma}_{33}$ along the thickness, $S = 2$, with three layers $(0°/90°/0°)$.

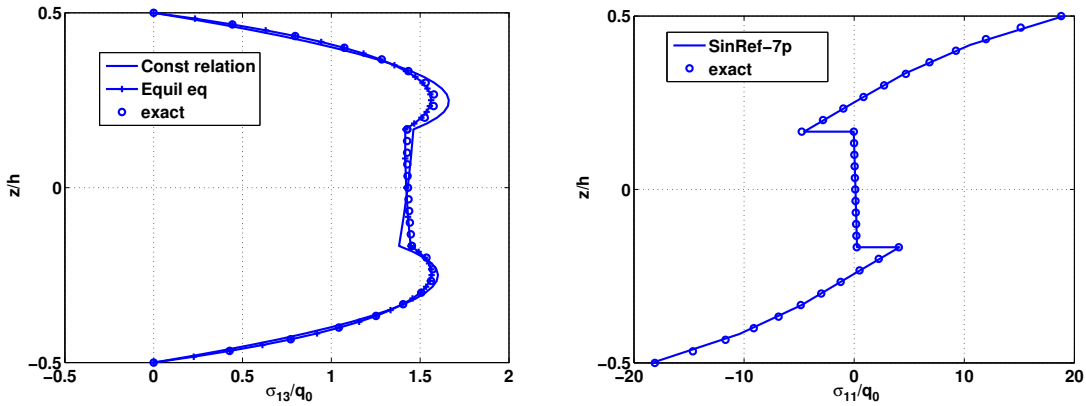

Figure 10. Distribution of $\bar{\sigma}_{13}$ and $\bar{\sigma}_{11}$ along the thickness, $S = 4$, $0°/90°/0°$, SinRef-7p.

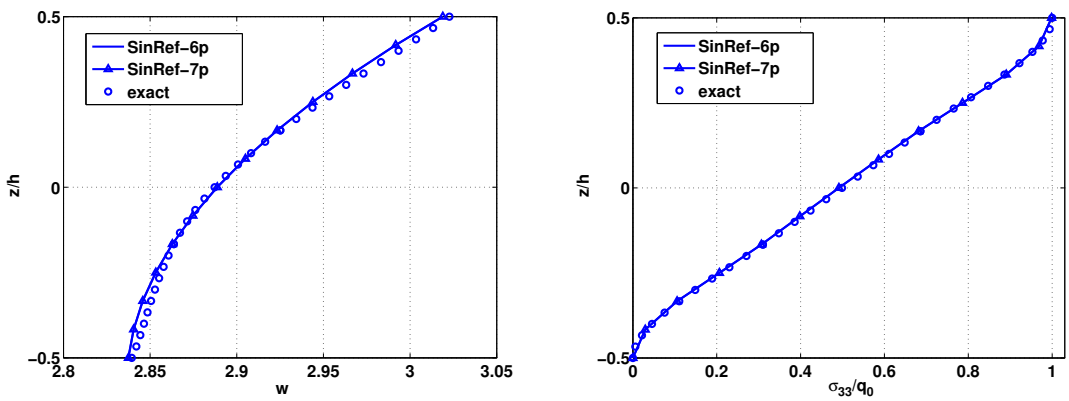

Figure 11. Distribution of $\bar{w}$ (left) and $\bar{\sigma}_{33}$ (right) along the thickness, $S = 4$, $0°/90°/0°$.

The error is less than 0.7% for in-plane and transverse displacements, and transverse shear stress with $S \geq 4$. The variation of the transverse shear stress calculated from the constitutive relation also gives good results. Moreover, for $S = 2$, Figure 11, left, shows that $\bar{w}$ is nonconstant. Note that the two

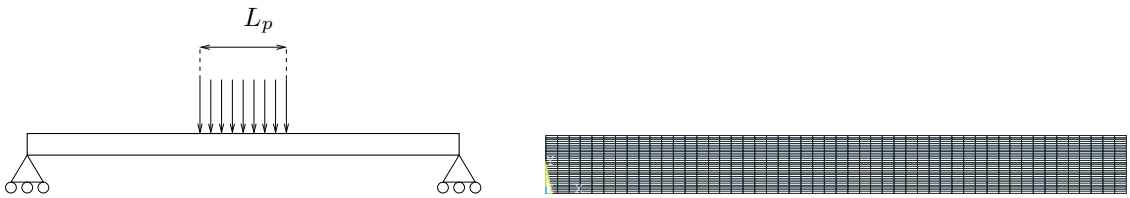

Figure 12. Left: beam under localized pressure. Right: the ANSYS mesh.

models with stretching effects take into account the nonsymmetrical variation of the transverse shear and the in-plane stress through the thickness (see Figure 8).

Bending analysis of laminated composite beam under localized pressure. This test is about simply supported symmetric and antisymmetric composite beams submitted to a localized pressure. It focuses on the capability of these elements to capture local behavior. It is detailed below.

Geometry: Composite cross-ply beam $(0°/90°/0°)$ and $(0°/90°)$ and $S = 4$; half of the beam is meshed. All layers have the same thickness.

Boundary conditions: Simply supported beam subjected to a transverse pressure $q(x_1) = q_0$ applied on a line located at the beam center and whose dimension is $L_p = L/8$ (see Figure 12).

Material properties: Same properties as on page 1136.

Mesh: $N = 16$.

Results: The reference solution is issued from a 2D elasticity analysis with a very refined mesh including 3800 DOFs in ANSYS. The element PLANE82 is used.

The results are shown in Table 8. We observe that the three models perform quite well with respect to the 2D solution except for the in-plane stress in the SinRef-c model. This is due to the nonsymmetrical results across the thickness which can not be taken into account in this model. From Figures 13 and 14, it can be noticed that the transverse displacement is nonconstant across the thickness. In all cases, the models including the transverse deformation are in excellent agreement with the reference solution.

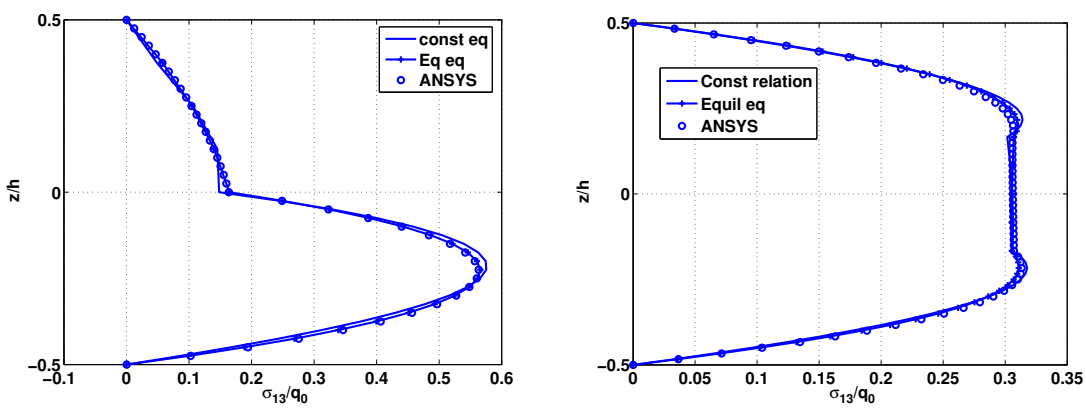

Figure 13. Distribution of $\bar{\sigma}_{13}$ along the thickness, $S = 4$, with two layers (left) and three layers (right), SinRef-7p, localized pressure.

		(0°/90°/0°)				(0°/90°)			
		(x_1, z)		error	ANSYS	(x_1, z)		error	ANSYS
SinRef-7p	$\bar{\sigma}_{13}$ direct	$(0, 0)$	0.3059	0.1%	0.3061	$(0, -h/4)$	0.5656	1%	0.5602
	$\bar{\sigma}_{13}$ equiv.eq	$(0, 0)$	0.3055	0.2%		$(0, -h/4)$	0.5616	0.2%	
	$\bar{\sigma}_{11}$	$(L/2, -h/2)$	6.4510	14%	5.6406	$(L/2, -h/2)$	9.8455	9%	8.9715
	$\bar{w}$	$(L/2, 0)$	0.7809	0.4%	0.7847	$(L/2, 0)$	1.2510	0.8%	1.2617
	$\bar{u}$	$(0, h/2)$	0.2131	1%	0.2165	$(0, h/2)$	1.0774	0.1%	1.0788
SinRef-6p	$\bar{\sigma}_{13}$ direct	$(0, 0)$	0.3084	0.7%	0.3061	$(0, -h/4)$	0.5117	8%	0.5602
	$\bar{\sigma}_{13}$ equiv.eq	$(0, 0)$	0.3048	0.4%		$(0, -h/4)$	0.5290	5%	
	$\bar{\sigma}_{11}$	$(L/2, -h/2)$	6.4195	13%	5.6406	$(L/2, -h/2)$	9.2047	2%	8.9715
	$\bar{w}$	$(L/2, 0)$	0.7809	0.4%	0.7847	$(L/2, 0)$	1.2310	2%	1.2617
	$\bar{u}$	$(0, h/2)$	0.2142	1%	0.2165	$(0, h/2)$	1.0871	0.7%	1.0788
SinRef-c	$\bar{\sigma}_{13}$ direct	$(0, 0)$	0.3082	0.7%	0.3061	$(0, -h/4)$	0.5211	7%	0.5602
	$\bar{\sigma}_{13}$ equiv.eq	$(0, 0)$	0.3051	0.3%		$(0, -h/4)$	0.5659	1%	
	$\bar{\sigma}_{11}$	$(L/2, -h/2)$	7.5326	33%	5.6406	$(L/2, -h/2)$	11.8810	32%	8.9715
	$\bar{w}$	$(L/2, 0)$	0.7969	1.5%	0.7847	$(L/2, 0)$	1.2451	1%	1.2617
	$\bar{u}$	$(0, h/2)$	0.2181	0.7%	0.2165	$(0, h/2)$	1.1259	4%	1.0788

Table 8. $S = 4$, with two and three layers, localized pressure.

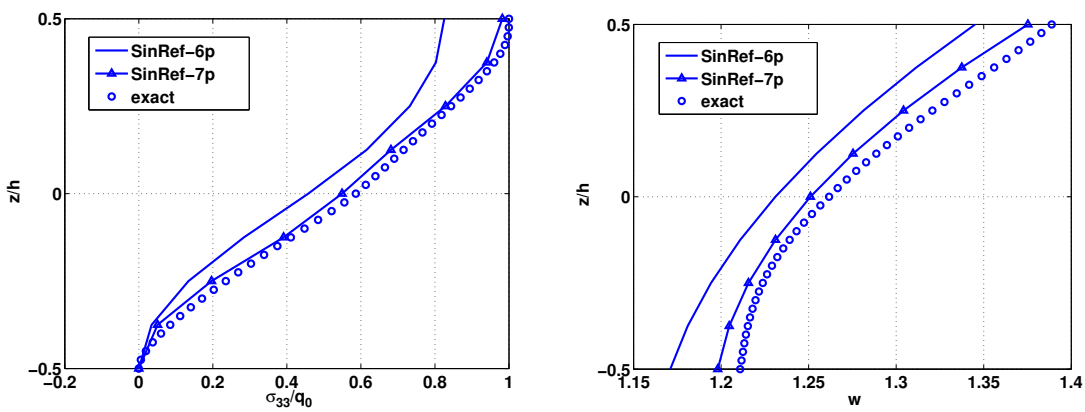

Figure 14. Distribution of $\bar{\sigma}_{33}$ and $\bar{w}$ along the thickness, $S = 4$, with two layers $(0°/90°)$, localized pressure.

As in the previous case, the SinRef-7p model improves results issued from the SinRef-6p model, especially for the transverse shear stress in the antisymmetric lay-up.

Bending analysis of a sandwich beam under uniform pressure. The test deals with a sandwich beam under uniform pressure with two different boundary conditions. Only the more accurate model, the SinRef-7p model, is used in this severe test. This example is detailed now.

Geometry: The 3-layer sandwich beam has graphite-epoxy faces and a soft core with thicknesses $0.1h$, $0.8h$, $0.1h$ and length to thickness ratios $S = 2.5$, $S = 5$, $S = 10$; half of the beam is meshed.

Boundary conditions: Simply supported or clamped-clamped (C-C) beam under an uniform pressure q_0.

Material properties (face): $E_{11} = 131.1\,\text{GPa}$, $E_{22} = E_{33} = 6.9\,\text{GPa}$, $G_{12} = 3.588\,\text{GPa}$, $G_{13} = 3.088\,\text{GPa}$, $G_{23} = 2.3322\,\text{GPa}$, $\nu_{12} = \nu_{13} = 0.32$, $\nu_{23} = 0.49$.

Material properties (core): $E_{11} = 0.2208\,\text{MPa}$, $E_{22} = 0.2001\,\text{MPa}$, $E_{33} = 2760\,\text{MPa}$, $G_{12} = 16.56\,\text{MPa}$, $G_{13} = 545.1\,\text{MPa}$, $G_{23} = 455.4\,\text{MPa}$, $\nu_{12} = 0.99$, $\nu_{13} = 0.00003$, $\nu_{23} = 0.00003$.

Mesh: $N = 16$.

Results: The results are presented in nondimensional form as

$$\bar{w} = 100 w Y_0 / h S^4 q_0, \quad \bar{\sigma}_{11} = \sigma_{11}/S^2 q_0, \quad \bar{\tau}_{13} = \tau_{13}/S q_0, \quad Y_0 = 6.9\,\text{GPa}.$$

They are compared with the available 2D exact solution from [Kapuria et al. 2004] and results from a commercial code with a very refined mesh including 3800 DOFs. This choice is justified by the convergence study given in Table 9 for a slenderness ratio $S = 2.5$. The error on the stresses with respect to the reference mesh (61000 DOFs) becomes negligible when the number of DOFs is greater than 3800.

Tables 10 and 11 show that the model is very efficient and accurate, even for the very thick case. Figure 15 gives the distribution of in-plane, transverse shear, and normal stresses through the thickness for the clamped-clamped beam with $S = 2.5$. These stresses are very well estimated, in particular the maximum transverse shear stress in the face and the asymmetrical maximum value due to the thickness and the load.

$\bar{\sigma}_{11}(L/2, -h/2)$	1%	0.5%	0.1%	0.03%	2.1000
$\bar{\sigma}_{13\,\max}$	12%	0.7%	0.7%	0.0%	0.8309
DOFs	700	2000	3800	15000	61000

Table 9. Convergence study (ANSYS), $S = 2.5$, C-C. Reference values are in the last column.

S			error	literature	ANSYS
2.5	$\bar{\sigma}_{13}(0, 0)$	0.4773	0.1%		0.4777
	$\bar{\sigma}_{11}(L/2, h/2)$	−3.2370	0.3%		−3.2285
	$\bar{\sigma}_{11}(L/2, -h/2)$	3.2686	1.1%		3.2318
	$\bar{w}(L/2, 0)$	25.5916	0.1%		25.5761
5	$\bar{\sigma}_{13}(0, 0)$	0.5153	0.2%	0.5144	0.5155
	$\bar{\sigma}_{11}(L/2, h/2)$	−1.9729	0.2%	−1.9698	−1.9655
	$\bar{\sigma}_{11}(L/2, -h/2)$	1.9727	0.2%	1.9689	1.9655
	$\bar{w}(L/2, 0)$	7.8804	0.0%	7.8778	7.8925
10	$\bar{\sigma}_{13}(0, 0)$	0.5346	0.1%	0.5338	0.5344
	$\bar{\sigma}_{11}(L/2, h/2)$	−1.6466	0.1%	−1.6451	−1.6441
	$\bar{\sigma}_{11}(L/2, -h/2)$	1.6466	0.1%	1.6449	1.6441
	$\bar{w}(L/2, 0)$	3.2416	0.2%	3.2486	3.2521

Table 10. Sandwich, uniform pressure, simply supported. Literature values are taken from [Kapuria et al. 2004].

S			error	ANSYS
2.5	$\bar{\sigma}_{13}(L/8,0)$	0.3280	0.5%	0.3263
	$\bar{\sigma}_{13}$ max	0.8038	3%	0.8310
	$\bar{\sigma}_{11}(L/2,h/2)$	-2.3326	7%	-2.1610
	$\bar{\sigma}_{11}(L/2,-h/2)$	2.0056	4%	2.1000
	$\bar{w}(L/2,0)$	20.2549	1.4%	20.5340
5	$\bar{\sigma}_{13}(L/8,0)$	0.3877	0.1%	0.3880
	$\bar{\sigma}_{11}(L/2,h/2)$	-0.9966	4%	-0.9520
	$\bar{\sigma}_{11}(L/2,-h/2)$	0.9237	1.7%	0.9398
	$\bar{w}(L/2,0)$	6.0218	1.1%	5.9550
10	$\bar{\sigma}_{13}(L/8,0)$	0.4120	0.1%	0.4125
	$\bar{\sigma}_{11}(L/2,h/2)$	-0.6351	2%	-0.6224
	$\bar{\sigma}_{11}(L/2,-h/2)$	0.6154	0.6%	0.6193
	$\bar{w}(L/2,0)$	1.8186	0.9%	1.8358

Table 11. Sandwich, uniform pressure, C-C. The tranverse shear stress is calculated at $x = L/8$ because the 2D finite element solution is not valid at a fixed edge.

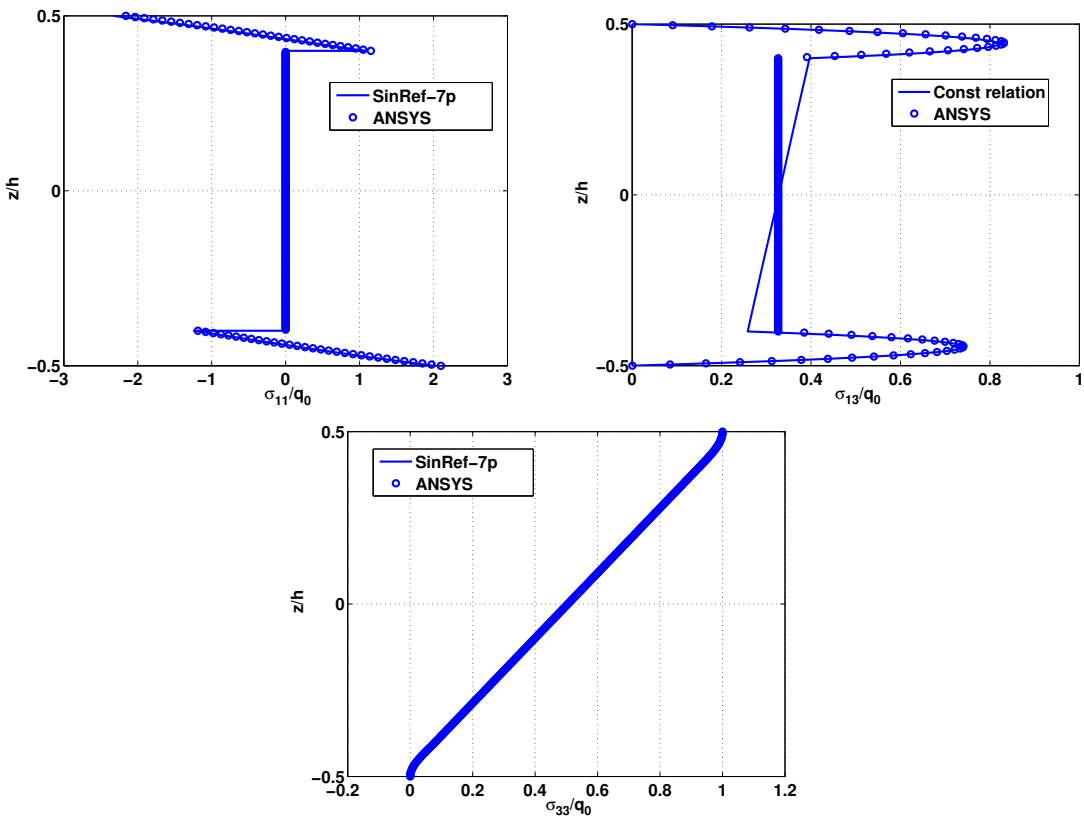

Figure 15. Distribution of $\bar{\sigma}_{11}$, $\bar{\sigma}_{13}$ and $\bar{\sigma}_{33}$ along the thickness, $S = 2.5$, sandwich, SinRef-7p, uniform pressure, C-C.

4. A thermomechanical problem

In this section, the accuracy of the present theory is assessed in thermomechanical analysis. The results are compared with the exact 2D thermoelasticity solution [Bhaskar et al. 1996]. The problem is described as follows:

Geometry: Composite cross-ply beam $(0°/90°/0°)$ and $(0°/90°)$, slenderness ratio S ranging from 4 to 100; half of the beam is meshed. All layers have the same thickness.

Boundary conditions: Simply supported beam subjected to the temperature field

$$T(x_1, z) = T_{\max} \frac{2z}{h} \sin \frac{\pi x_1}{L}. \tag{22}$$

It corresponds to a cylindrical bending.

Material properties: Same properties as on page 1136, plus $\alpha_T = 1125\alpha_L$, where α_L, α_T are the thermal expansion coefficients in the fiber and normal direction.

Mesh: $N = 8$.

Results: As in reference [Carrera 2000a], we define the dimensionless quantities:

$$\bar{u} = \frac{u_1}{\alpha_L T_{\max} L}, \qquad \bar{w} = \frac{h u_3}{\alpha_L T_{\max} L^2}, \qquad \bar{\sigma}_{11} = \frac{\sigma_{11}}{\alpha_L E_T T_{\max}}, \qquad \bar{\sigma}_{13} = \frac{\sigma_{13}}{\alpha_L E_T T_{\max}}. \tag{23}$$

The reference results have been obtained upon an extension to the thermomechanical problem of the exact Pagano solution given in [Pagano 1969].

The numerical results for deflection, in-plane displacement, shear stress, and in-plane stress are given in Tables 12–14 and 15–17 for two and three layers, respectively. These examples show clearly the necessity to take into account the transverse normal deformation in the model. In fact, the improvement is significant for the SinRef-6p and SinRef-7p models compared to the SinRef-c one.

			$\bar{u}(0, h/2)$				
S	SinRef-7p	error	SinRef-6p	error	SinRef-c	error	exact
4	155.1	0.2%	156.60	0.8%	153.39	1%	155.36
10	114.22	0.03%	114.35	0.1%	111.88	2%	114.18
50	104.50	$< 0.01\%$	104.50	$< 0.01\%$	101.93	2%	104.50
100	104.18	0.01%	104.18	$< 0.01\%$	101.60	2%	104.19
			$\bar{w}(L/2, 0)$				
S	SinRef-7p	error	SinRef-6p	error	SinRef-c	error	exact
4	42.652	0.5%	41.302	3%	45.882	7%	42.889
10	43.285	0.01%	43.023	0.6%	42.191	2%	43.293
50	43.158	$< 0.01\%$	43.146	0.03%	41.314	4%	43.161
100	43.152	$< 0.01\%$	43.149	0.01%	41.286	4%	43.155

Table 12. $\bar{u}(0, h/2)$ and $\bar{w}(L/2, 0)$ for different values of S, with two layers $(0°/90°)$.

$\bar{\sigma}_{13}(0, -h/4)$													
	SinRef-7p				SinRef-6p				SinRef-c				
S	direct	error	equil.eq	error	direct	error	equil.eq	error	direct	error	equil.eq	error	exact
4	136.350	3%	129.610	1%	109.820	16%	134.320	2%	119.600	9%	133.170	1%	131.730
10	68.707	1%	67.422	0.8%	55.351	18%	67.834	0.2%	59.742	12%	68.341	0.5%	67.964
50	14.430	0.6%	14.240	0.6%	11.611	18%	14.244	0.6%	12.519	12%	14.391	0.4%	14.333
100	7.225	0.6%	7.132	0.6%	5.814	19%	7.133	0.6%	6.269	12%	7.207	0.3%	7.179

Table 13. $\bar{\sigma}_{13}(0, -h/4)$ for different values of S, with two layers (0°/90°).

$\bar{\sigma}_{11}(L/2, -h/2)$							
S	SinRef-7p	error	SinRef-6p	error	SinRef-c	error	exact
4	2044.1	2%	2075.4	4%	1774.5	11%	1994.7
10	2142.4	0.6%	2150.1	1%	2115.3	0.6%	2129.0
50	2179.8	0.4%	2180.1	0.4%	2197.1	1%	2170.2
100	2181.1	0.4%	2181.2	0.4%	2199.8	1%	2171.7

Table 14. $\bar{\sigma}_{11}(L/2, -h/2)$ for different values of S, with two layers (0°/90°).

$\bar{u}(0, h/2)$							
S	SinRef-7p	error	SinRef-6p	error	SinRef-c	error	exact
4	7.5399	0.9%	7.5262	0.7%	0.2608	96%	7.4696
10	5.0069	0.05%	5.0013	0.1%	0.7346	85%	5.0095
50	4.4667	$< 0.01\%$	4.4665	0.01%	0.8622	80%	4.4670
100	4.4493	$< 0.01\%$	4.4492	$< 0.01\%$	0.8665	80%	4.4494
$\bar{w}(L/2, 0)$							
S	SinRef-7p	error	SinRef-6p	error	SinRef-c	error	exact
4	3.6285	0.3%	3.6272	0.3%	0.2332	93%	3.6156
10	1.8935	0.01%	1.8919	0.08%	0.3762	80%	1.8934
50	2.7924	$< 0.01\%$	2.7924	$< 0.01\%$	0.5449	80%	2.7924
100	2.8197	$< 0.01\%$	2.8197	$< 0.01\%$	0.5506	80%	2.8197

Table 15. $\bar{u}(0, h/2)$ and $\bar{w}(L/2, 0)$ for different values of S, with three layers (0°/90°/0°).

	SinRef-7p				SinRef-6p				SinRef-c				
S	direct	error	equil.eq	error	direct	error	equil.eq	error	direct	error	equil.eq	error	exact
4	21.4280	0.04%	21.7350	1.5%	20.2340	5%	21.7010	1.3%	6.8092	68%	14.3210	33%	21.4178
10	7.1544	0.1%	7.2837	2%	6.2585	12%	7.2771	1.8%	3.7459	47%	6.5851	7%	7.1436
50	1.3522	0.1%	1.3778	2%	1.1538	14%	1.3777	2%	0.8040	40%	1.3629	1%	1.3497
100	0.6748	0.1%	0.6876	2%	0.5753	14%	0.6875	2%	0.4029	40%	0.6822	1%	0.6735

Table 16. $\bar{\sigma}_{13}(0, 0)$ (max) for different values of S, with three layers (0°/90°/0°).

	$\bar{\sigma}_{11}(L/2, -h/2)$						
S	SinRef-7p	error	SinRef-6p	error	SinRef-c	error	exact
4	289.17	2.8%	288.10	2%	4.4627	98%	281.11
10	88.63	1.4%	88.19	1%	32.96	62%	87.41
50	45.83	2.5%	45.80	2%	43.0390	3%	44.70
100	44.44	2.6%	44.44	2%	43.3780	0.1%	43.31

Table 17. $\bar{\sigma}_{11}(L/2, -h/2)$ for different values of S, with three layers $(0°/90°/0°)$.

Note that the SinRef-7p results are in excellent agreement with the exact solution. The error is less than 3% regardless of the length to thickness ratio for both displacements and stresses, and even for the transverse shear stress deduced from the constitutive relation. Figures 16–20 show that the distribution of these quantities are similar to the reference solution, in particular for the thick beam.

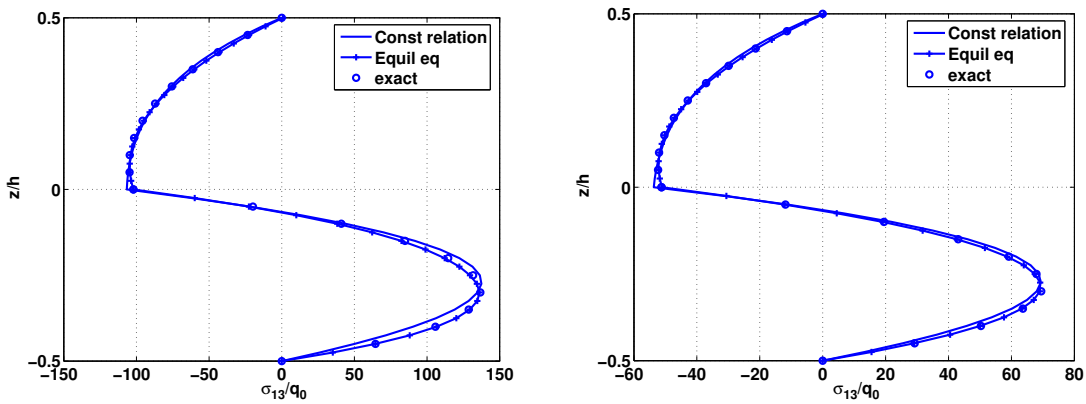

Figure 16. Distribution of $\bar{\sigma}_{13}$ along the thickness, $S = 4$ (left) and $S = 20$ (right), with two layers $(0°/90°)$, SinRef-7p model.

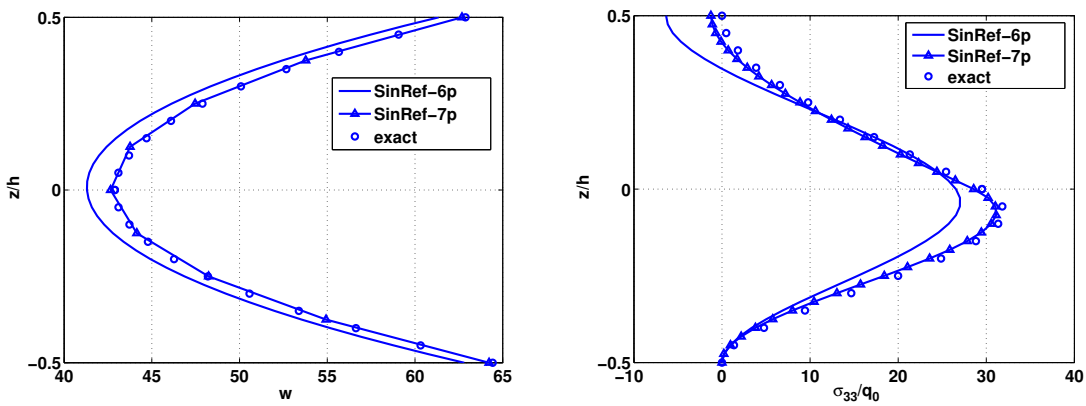

Figure 17. Distribution of $\bar{w}$ (left) and $\bar{\sigma}_{33}$ (right) along the thickness, $S = 4$, with two layers $(0°/90°)$.

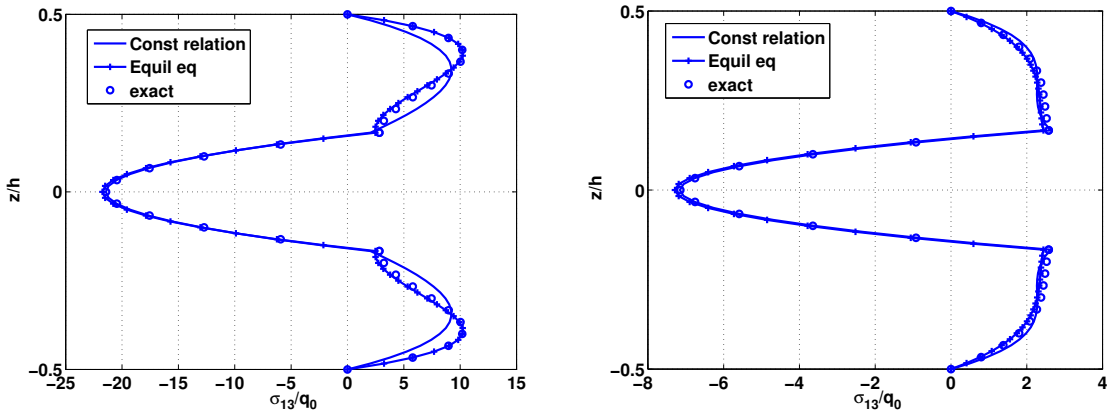

Figure 18. Distribution of $\bar{\sigma}_{13}$ along the thickness, $S = 4$ (left) and $S = 10$ (right), with three layers $(0°/90°/0°)$, SinRef-7p model.

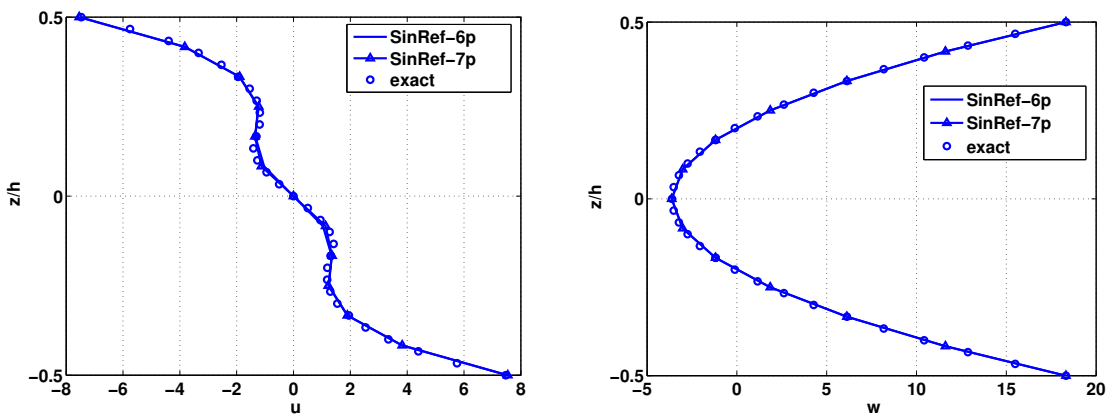

Figure 19. Distribution of $\bar{u}$ (left) and $\bar{w}$ (right) along the thickness, $S = 4$, with three layers $(0°/90°/0°)$.

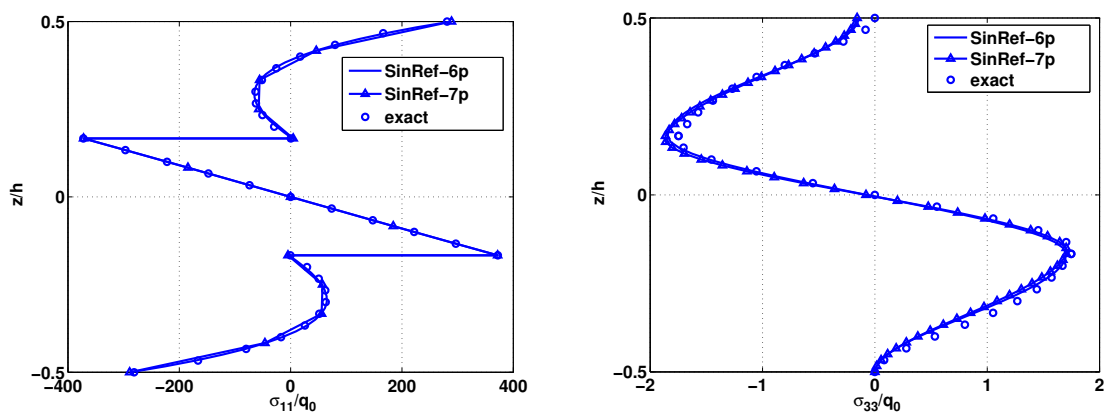

Figure 20. Distribution of $\bar{\sigma}_{11}$ (left) and $\bar{\sigma}_{33}$ (right) along the thickness, $S = 4$, with three layers $(0°/90°/0°)$.

Concerning the SinRef-6p model, the percentage error is close to the previous one except for the transverse shear stress where it is more important. However, notice that only the quantity calculated directly from the constitutive relation is involved. For the thick beam, the distribution of the transverse normal stress is in good agreement with the reference solution for the two cases (Figures 17, right, and 20, right). However, the accuracy of this quantity calculated by the SinRef-7p model is improved (see Figure 17, right). The same holds for the transverse displacement (see Figure 17, left).

5. Conclusion

In this article, two new numerical models, denoted SinRef-6p and SinRef-7p, have been presented and evaluated through different benchmarks under mechanical and thermomechanical loading. Special attention is pointed towards the transverse normal stress effect, which plays an important role for thick beams and coupled problems. Each of the two models consists in a three-node multilayered (sandwich and laminated) beam finite element for static analysis with a parabolic distribution of transverse displacement. Based on the sine equivalent single layer model, a third-order kinematic per layer is added, improving the bending description for thick beams. There is no need for transverse shear correction factors and all the interface and boundary conditions are exactly satisfied. So, this approach has a strong physical meaning. Finally, the number of unknowns is independent of the number of layers.

Several numerical evaluations have proved that this model has very good properties in the field of finite elements. Convergence velocity is high and accurate results are obtained for very thick and thin cases. So, these finite elements are simple and efficient for a low cost, compared to layerwise approach or plane elasticity model in commercial software. This study shows the necessity of taking into account the transverse normal effect which cannot be neglected, in particular for coupled thermomechanical problems. This approach allows us to calculate the transverse shear stress directly by the constitutive relation with a very satisfactory accuracy.

Based on these promising results, an extension to plates, shells and piezoelastic coupling will be investigated.

References

[Aitharaju and Averill 1999] V. R. Aitharaju and R. C. Averill, "C^0 zig-zag finite element for analysis of laminated composite beams", *J. Eng. Mech.* (*ASCE*) **125**:3 (1999), 323–330.

[Ali et al. 1999] J. S. M. Ali, K. Bhaskar, and T. K. Varadan, "A new theory for accurate thermal/mechanical flexural analysis of symmetric laminated plates", *Compos. Struct.* **45**:3 (1999), 227–232.

[Ambartsumyan 1969] S. A. Ambartsumyan, *Theory of anisotropic plates*, edited by J. E. Ashton, Technomic, Stamford, CT, 1969. Translated from Russian by T. Cheron.

[Averill and Yip 1996] R. C. Averill and Y. C. Yip, "Thick beam theory and finite element model with zig-zag sublaminate approximations", *AIAA J.* **34**:8 (1996), 1627–1632.

[Barbero et al. 1990] E. J. Barbero, J. N. Reddy, and J. Teply, "An accurate determination of stresses in thick laminates using a generalized plate theory", *Int. J. Numer. Methods Eng.* **29**:1 (1990), 1–14.

[Barut et al. 2001] A. Barut, E. Madenci, J. Heinrich, and A. Tessler, "Analysis of thick sandwich construction by a {3, 2}-order theory", *Int. J. Solids Struct.* **38**:34–35 (2001), 6063–6077.

[Basset 1890] A. Basset, "On the extension and flexure of cylindrical and spherical thin elastic shells", *Phil. Trans. R. Soc. A* **181** (1890), 433–480.

[Bhaskar and Varadan 1989] K. Bhaskar and T. K. Varadan, "Refinement of higher-order laminated plate theories", *AIAA J.* **27**:12 (1989), 1830–1831.

[Bhaskar et al. 1996] K. Bhaskar, T. K. Varadan, and J. S. M. Ali, "Thermoelastic solutions for orthotropic and anisotropic composite laminates", *Compos. B Eng.* **27**:5 (1996), 415–420.

[Carrera 1999] E. Carrera, "A study of transverse normal stress effect on vibration of multilayered plates and shells", *J. Sound Vib.* **225**:5 (1999), 803–829.

[Carrera 2000a] E. Carrera, "An assessment of mixed and classical theories for the thermal stress analysis of orthotropic multilayered plates", *J. Therm. Stresses* **23**:9 (2000), 797–831.

[Carrera 2000b] E. Carrera, "A priori vs. a posteriori evaluation of transverse stresses in multilayered orthotropic plates", *Compos. Struct.* **48**:4 (2000), 245–260.

[Carrera 2002] E. Carrera, "Theories and finite elements for multilayered, anisotropic, composite plates and shells", *Arch. Comput. Methods Eng.* **9**:2 (2002), 87–140.

[Carrera 2003] E. Carrera, "Historical review of zig-zag theories for multilayered plates and shells", *Appl. Mech. Rev.* (*ASME*) **56**:3 (2003), 287–308.

[Carrera 2004] E. Carrera, "On the use of the Murakami's zig-zag function in the modeling of layered plates and shells", *Comput. Struct.* **82**:7–8 (2004), 541–554.

[Carrera and Brischetto 2008] E. Carrera and S. Brischetto, "Analysis of thickness locking in classical, refined and mixed multilayered plate theories", *Compos. Struct.* **82**:4 (2008), 549–562.

[Chaudhri 1986] R. A. Chaudhri, "An equilibrium method for prediction of transverse shear stresses in a thick laminated plate", *Comput. Struct.* **23**:2 (1986), 139–146.

[Cho and Parmerter 1993] M. Cho and R. R. Parmerter, "Efficient higher order composite plate theory for general lamination configurations", *AIAA J.* **31**:7 (1993), 1299–1306.

[Cook and Tessler 1998] G. M. Cook and A. Tessler, "A {3, 2}-order bending theory for laminated composite and sandwich beams", *Compos. B Eng.* **29**:5 (1998), 565–576.

[Dau et al. 2006] F. Dau, O. Polit, and M. Touratier, "C^1 plate and shell finite elements for geometrically nonlinear analysis of multilayered structures", *Comput. Struct.* **84**:19–20 (2006), 1264–1274.

[Flanagan 1994] G. Flanagan, "A general sublaminate analysis method for determining strain energy release rates in composites", pp. 381–389 in 35*th AIAA/ASME/ASCE/AHS/ASC Structures, Structural Dynamics, and Materials Conference* (Hilton Head, SC, 1994), AIAA, Reston, VA, 1994. Paper #1994-1356.

[Ganapathi et al. 1999] M. Ganapathi, B. P. Patel, P. Boisse, and O. Polit, "Flexural loss factors of sandwich and laminated composite beams using linear and nonlinear dynamic analysis", *Compos. B Eng.* **30**:3 (1999), 245–256.

[Gaudenzi et al. 1995] P. Gaudenzi, R. Barboni, and A. Mannini, "A finite element evaluation of single-layer and multi-layer theories for the analysis of laminated plates", *Compos. Struct.* **30**:4 (1995), 427–440.

[Gherlone and di Sciuva 2007] M. Gherlone and M. di Sciuva, "Thermo-mechanics of undamaged and damaged multilayered composite plates: a sub-laminates finite approach", *Comput. Struct.* **81**:1 (2007), 125–136.

[Han and Hoa 1993] J. Han and S. V. Hoa, "A three-dimensional multilayer composite finite element for stress analysis of composite laminates", *Int. J. Numer. Methods Eng.* **36**:22 (1993), 3903–3914.

[Heller and Swift 1971] R. Heller and G. Swift, "Solutions for the multilayer Timoshenko beam", Technical Report VPI-E-71-12, Virginia Polytechnic Institute, Blacksburg, VA, 1971.

[Icardi 2001] U. Icardi, "Higher-order zig-zag model for analysis of thick composite beams with inclusion of transverse normal stress and sublaminates approximations", *Compos. B Eng.* **32**:4 (2001), 343–354.

[Kant and Gupta 1988] T. Kant and A. Gupta, "A finite element model for a higher-order shear-deformable beam theory", *J. Sound Vib.* **125**:2 (1988), 193–202.

[Kant and Swaminathan 2000] T. Kant and K. Swaminathan, "Estimation of transverse/interlaminar stresses in laminated composites: a selective review and survey of current developments", *Compos. Struct.* **49**:1 (2000), 65–75.

[Kant and Swaminathan 2002] T. Kant and K. Swaminathan, "Analytical solutions for the static analysis of laminated composite and sandwich plates based on a higher order refined theory", *Compos. Struct.* **56**:4 (2002), 329–344.

[Kant et al. 1997] T. Kant, S. R. Marur, and G. S. Rao, "Analytical solution to the dynamic analysis of laminated beams using higher order refined theory", *Compos. Struct.* **40**:1 (1997), 1–9.

[Kapuria et al. 2003] S. Kapuria, P. C. Dumir, and A. Ahmed, "An efficient higher order zigzag theory for composite and sandwich beams subjected to thermal loading", *Int. J. Solids Struct.* **40**:24 (2003), 6613–6631.

[Kapuria et al. 2004] S. Kapuria, P. C. Dumir, and N. K. Jain, "Assessment of zigzag theory for static loading, buckling, free and forced response of composite and sandwich beams", *Compos. Struct.* **64**:3–4 (2004), 317–327.

[Kärger et al. 2006] L. Kärger, A. Wetzel, R. Rolfes, and K. Rohwer, "A three-layered sandwich element with improved transverse shear stiffness and stresses based on FSDT", *Comput. Struct.* **84**:13–14 (2006), 843–854.

[Kim and Cho 2007] J.-S. Kim and M. Cho, "Enhanced first-order theory based on mixed formulation and transverse normal effect", *Int. J. Solids Struct.* **44**:3–4 (2007), 1256–1276.

[Lee et al. 1992] C.-Y. Lee, D. Liu, and X. Lu, "Static and vibration analysis of laminated composite beams with an interlaminar shear stress continuity theory", *Int. J. Numer. Methods Eng.* **33**:2 (1992), 409–424.

[Li and Liu 1997] X. Li and D. Liu, "Generalized laminate theories based on double superposition hypothesis", *Int. J. Numer. Methods Eng.* **40**:7 (1997), 1197–1212.

[Librescu 1967] L. Librescu, "On the theory of anisotropic elastic shells and plates", *Int. J. Solids Struct.* **3**:1 (1967), 53–68.

[Liu and Soldatos 2002] S. Liu and K. P. Soldatos, "On the prediction improvement of transverse stress distributions in cross-ply laminated beams: advanced versus conventional beam modelling", *Int. J. Mech. Sci.* **44**:2 (2002), 287–304.

[Lo et al. 1977] K. Lo, R. Christensen, and F. Wu, "A higher-order theory of plate deformation, II: Laminated plates", *J. Appl. Mech.* (*ASME*) **44** (1977), 669–676.

[Matsunaga 2002] H. Matsunaga, "Assessment of a global higher-order deformation theory for laminated composite and sandwich plates", *Compos. Struct.* **56**:3 (2002), 279–291.

[Mau 1973] S. Mau, "A refined laminate plate theory", *J. Appl. Mech.* (*ASME*) **40** (1973), 606–607.

[Mindlin 1951] R. Mindlin, "Influence of rotatory inertia and shear on flexural motions of isotropic, elastic plates", *J. Appl. Mech.* (*ASME*) **18** (1951), 31–38.

[Mittelstedt and Becker 2007] C. Mittelstedt and W. Becker, "Free-edge effects in composite laminates", *Appl. Mech. Rev.* (*ASME*) **60**:5 (2007), 217–244.

[Murakami 1986] H. Murakami, "Laminated composite plate theory with improved in-plane responses", *J. Appl. Mech.* (*ASME*) **53** (1986), 661–666.

[Noor and Burton 1990] A. K. Noor and W. S. Burton, "Assessment of computational models for multilayered composite shells", *Appl. Mech. Rev.* (*ASME*) **43**:4 (1990), 67–97.

[Noor and Malik 1999] A. K. Noor and M. Malik, "Accurate determination of transverse normal stresses in sandwich panels subjected to thermomechanical loadings", *Comput. Methods Appl. Mech. Eng.* **178**:3–4 (1999), 431–443.

[Pagano 1969] N. J. Pagano, "Exact solutions for composite laminates in cylindrical bending", *J. Compos. Mater.* **3**:3 (1969), 398–411.

[Pagano 1970] N. J. Pagano, "Exact solutions for rectangular bidirectional composites and sandwich plates", *J. Compos. Mater.* **4**:1 (1970), 20–34.

[Pai and Palazotto 2001] P. F. Pai and A. N. Palazotto, "A higher-order sandwich plate theory accounting for 3-D stresses", *Int. J. Solids Struct.* **38**:30–31 (2001), 5045–5062.

[Polit and Touratier 2002] O. Polit and M. Touratier, "A multilayered/sandwich triangular finite element applied to linear and non-linear analysis", *Compos. Struct.* **58**:1 (2002), 121–128.

[Polit et al. 1994] O. Polit, M. Touratier, and P. Lory, "A new eight-node quadrilateral shear-bending plate finite element", *Int. J. Numer. Methods Eng.* **37**:3 (1994), 387–411.

[Rao and Desai 2004] M. K. Rao and Y. M. Desai, "Analytical solutions for vibrations of laminated and sandwich plates using mixed theory", *Compos. Struct.* **63**:3–4 (2004), 361–373.

[Reddy 1984] J. N. Reddy, "A simple higher-order theory for laminated composite plates", *J. Appl. Mech.* (*ASME*) **51**:4 (1984), 745–752.

[Reddy 1989] J. N. Reddy, "On refined computational models of composite laminates", *Int. J. Numer. Methods Eng.* **27**:2 (1989), 361–382.

[Reddy 1997] J. N. Reddy, *Mechanics of laminated composite plates: theory and analysis*, CRC Press, Boca Raton, FL, 1997.

[Robaldo 2006] A. Robaldo, "Finite element analysis of the influence of temperature profile on thermoelasticity of multilayered plates", *Comput. Struct.* **84**:19–20 (2006), 1236–1246.

[Rohwer et al. 2001] K. Rohwer, R. Rolfes, and H. Sparr, "Higher-order theories for thermal stresses in layered plates", *Int. J. Solids Struct.* **38**:21 (2001), 3673–3687.

[Rolfes et al. 1998] R. Rolfes, A. K. Noor, and H. Sparr, "Evaluation of transverse thermal stresses in composite plates based on first-order shear deformation theory", *Comput. Methods Appl. Mech. Eng.* **167**:3–4 (1998), 355–368.

[di Sciuva 1986] M. di Sciuva, "Bending, vibration and buckling of simply supported thick multilayered orthotropic plates: an evaluation of a new displacement model", *J. Sound Vib.* **105**:3 (1986), 425–442.

[di Sciuva and Icardi 2001] M. di Sciuva and U. Icardi, "Numerical assessment of the core deformability effect on the behavior of sandwich beams", *Compos. Struct.* **52**:1 (2001), 41–53.

[Shimpi and Ainapure 2001] R. P. Shimpi and A. V. Ainapure, "A beam finite element based on layerwise trigonometric shear deformation theory", *Compos. Struct.* **53**:2 (2001), 153–162.

[Soldatos and Watson 1997] K. P. Soldatos and P. Watson, "A general theory for the accurate stress analysis of homogeneous and laminated composite beams", *Int. J. Solids Struct.* **34**:22 (1997), 2857–2885.

[Srinivas 1973] S. Srinivas, "A refined analysis of laminated composites", *J. Sound Vib.* **30**:4 (1973), 495–507.

[Subramanian 2001] P. Subramanian, "Flexural analysis of symmetric laminated composite beams using c^1 finite element", *Compos. Struct.* **54**:1 (2001), 121–126. Technical note.

[Subramanian 2006] P. Subramanian, "Dynamic analysis of laminated composite beams using higher order theories and finite elements", *Compos. Struct.* **73**:3 (2006), 342–353.

[Swaminathan and Patil 2007] K. Swaminathan and S. Patil, "Higher order refined computational model with 12 degrees of freedom for the stress analysis of antisymmetric angle-ply plates: analytical solutions", *Compos. Struct.* **80**:4 (2007), 595–608.

[Swift and Heller 1974] G. Swift and R. Heller, "Layered beam analysis", *J. Eng. Mech.* (*ASCE*) **100** (1974), 267–282.

[Sze et al. 1998] K. Y. Sze, R. Chen, and Y. K. Cheung, "Finite element model with continuous transverse shear stress for composite laminates in cylindrical bending", *Finite Elem. Anal. Des.* **31**:2 (1998), 153–164.

[Tahani 2007] M. Tahani, "Analysis of laminated composite beams using layerwise displacement theories", *Compos. Struct.* **79**:4 (2007), 535–547.

[Tanigawa et al. 1989] Y. Tanigawa, H. Murakami, and Y. Ootao, "Transient thermal stress analysis of a laminated composite beam", *J. Therm. Stresses* **12**:1 (1989), 25–39.

[Tessler et al. 2001] A. Tessler, M. S. Annett, and G. Gendron, "A {1, 2}-order plate theory accounting for three-dimensional thermoelastic deformations in thick composite and sandwich laminates", *Compos. Struct.* **52**:1 (2001), 67–84.

[Touratier 1991] M. Touratier, "An efficient standard plate theory", *Int. J. Eng. Sci.* **29**:8 (1991), 901–916.

[Touratier 1992a] M. Touratier, "A generalization of shear deformation theories for axisymmetric multilayered shells", *Int. J. Solids Struct.* **29**:11 (1992), 1379–1399.

[Touratier 1992b] M. Touratier, "A refined theory of laminated shallow shells", *Int. J. Solids Struct.* **29**:11 (1992), 1401–1415.

[Vidal and Polit 2006] P. Vidal and O. Polit, "A thermomechanical finite element for the analysis of rectangular laminated beams", *Finite Elem. Anal. Des.* **42**:10 (2006), 868–883.

[Vidal and Polit 2008] P. Vidal and O. Polit, "A family of sinus finite elements for the analysis of rectangular laminated beams", *Compos. Struct.* **84**:1 (2008), 56–72.

[Vidal and Polit 2009] P. Vidal and O. Polit, "Assessment of the refined sinus model for the non-linear analysis of composite beams", *Compos. Struct.* **87**:4 (2009), 370–381.

[Vinayak et al. 1996] R. U. Vinayak, G. Prathap, and B. P. Naganarayana, "Beam elements based on a higher order theory, I: Formulation and analysis of performance", *Comput. Struct.* **58**:4 (1996), 775–789.

[Whitney 1969] J. M. Whitney, "The effect of transverse shear deformation on the bending of laminated plates", *J. Compos. Mater.* **3**:3 (1969), 534–547.

[Whitney and Sun 1973] J. M. Whitney and C. T. Sun, "A higher order theory for extensional motion of laminated composites", *J. Sound Vib.* **30**:1 (1973), 85–97.

[Wu et al. 2005] Z. Wu, R. Chen, and W. Chen, "Refined laminated composite plate element based on global-local higher-order shear deformation theory", *Compos. Struct.* **70**:2 (2005), 135–152.

[Yang et al. 1966] P. C. Yang, C. H. Norris, and Y. Stavsky, "Elastic wave propagation in heterogeneous plates", *Int. J. Solids Struct.* **2**:4 (1966), 665–684.

[Zhang and Kim 2005] Y. X. Zhang and K. S. Kim, "A simple displacement-based 3-node triangular element for linear and geometrically nonlinear analysis of laminated composite plates", *Comput. Methods Appl. Mech. Eng.* **194**:45–47 (2005), 4607–4632.

[Zhang and Yang 2009] Y. X. Zhang and C. H. Yang, "Recent developments in finite elements analysis for laminated composite plates", *Compos. Struct.* **88**:1 (2009), 147–157.

[Zhen and Wanji 2007] W. Zhen and C. Wanji, "Refined global-local higher-order theory and finite element for laminated plates", *Int. J. Numer. Methods Eng.* **69**:8 (2007), 1627–1670.

Received 16 Dec 2008. Revised 26 Mar 2009. Accepted 27 May 2009.

PHILIPPE VIDAL: philippe.vidal@u-paris10.fr
LMpX, Université Paris Ouest, 50 rue de Sèvres, 92410 Ville d'Avray, France

OLIVIER POLIT: olivier.polit@u-paris10.fr
LMpX, Université Paris Ouest, 50 rue de Sèvres, 92410 Ville d'Avray, France